Applied Energy, Volume 283, February 2021, Article number 116374
DOI:10.1016/j.apenergy.2020.116374

Techno-economic design of energy systems for airport electrification: a hydrogen-solar-storage integrated microgrid solution

Yue Xiang[a], Hanhu Cai[a], Junyong Liu[a], Xin Zhang[b*]

[a] College of Electrical Engineering, Sichuan University, Chengdu 610065, China
[b] Centre for Energy Systems and Strategy, Power and Energy Theme, Cranfield University, United Kingdom
*Corresponding author: xin.zhang@cranfield.ac.uk

ABSTRACT: Can aviation really become less polluting? The electrification of airport energy system as a micro-grid is a promising solution to achieve zero emission airport operation, however such electrification approach presents the engineering challenge of integrating new energy resources, such as hydrogen supply and solar energy as attractive options to decarbonize the present system. This paper explores the techno-economic benefits of integrating hydrogen supply, electric auxiliary power unit (APU) of aircraft, electric vehicles, photovoltaic energy (PV), and battery storage system into electrified airport energy system. The hydrogen fuel cell generation provides great flexibility to supply aircraft at remote stands, and reduces the carbon emissions caused by traditional fuel-powered APU. A mixed integer linear programming optimization method based on life cycle theory is developed for capacity sizing of hydrogen energy system, PV and battery storage, with the multi-objectives of minimizing the total economic costs and maximizing environmental benefits of the proposed airport microgrid system. Case studies have been conducted by five different energy integration scenarios with techno-economic and environmental assessments to quantify the benefits of integrating hydrogen and renewable energy into airport. Compared with the benchmark scenarios, the integration of hydrogen energy system reduced the total annual cost and carbon emissions by 41.6% and 67.29%, respectively. Finally, sensitivity analysis of key system parameters such as solar irradiance, carbon tax, hydrogen system investment costs and electricity price have been investigated to inform the design of hydrogen-solar-storage integrated energy system for future airport electrification.

KEYWORDS: multi-energy system, microgrid, airport, electrification, PV, hydrogen, battery, techno-economic analysis

1. INTRODUCTION

1.1Background and challenges of airport electrification

Transportation is responsible for 24% of direct CO2 emissions from fuel combustion. Although aviation (air transport) is currently responsible for about 3% of the total CO2 emissions (IEA, 2018), the sector is growing at a fast rate of 6% annually [1]. Due to the global impacted coronavirus pandemic, the air travelling restrictions have led to a significant reduced in carbon emissions in aviation sector in 2020. However, we consider this pandemic to have temporary impacts on carbon

emissions which does not lead to a long-term sustainable aviation. Aviation industry mostly consumes fossil fuels, which is more difficult to be decarbonized than road and rail. Internationally, the complexity and need of aviation decarbonization have initiated policies and countermeasures in order to solve the environmental challenge of aviation industry by governments and relevant organizations [2]. For example, the European Union (EU) proposes Flightpath 2050 [3] agenda for a reduction of 90% in NOx-emissions, and 75% in CO2-emissions, and all airport ground operation is required to be emission free. The Civil Aviation Administration of China (CAAC) has announced "13th Five-Year Plan" for civil aviation [4] to target carbon emissions reduction by at least 4% compared to the previous five-year plan. One promising approach to achieve low-carbon aviation goals is through electrification, which has been put on the agenda by many airlines and manufactures to adopt electric aircraft and hybrid-electric aircraft [5]. However, some technical issues such as battery energy density make it difficult to realize the electrification of wide-body and long-haul fight. Therefore, our research focuses on the early feasibility of ground service equipment (GSE) electrification in airports, mainly reflected in two aspects: i) Ground vehicles in airport are fully electrified, such as passenger shuttle bus, aircraft tractors, aircraft guided vehicles, service vehicles, freight trailers, forklifts, etc; ii) Ground power unit (GPU) is used to power the aircraft to replace the operation of the auxiliary power unit (APU) when the aircraft is on the ground, namely APU alternative.

However, there are two potential challenges in power grid expansion to supply extra electricity for airport electrification: i) With the electrification of airplanes and ground service vehicles, the energy supply to meet future electric demand of the airport has become increasingly challenging. For examples, the aircraft APU is required to be supplied by airport energy system, and EV charging becomes an additional requirement for airport to provide energy supply. In order to satisfy the "supply-demand" balance of airport energy system, traditional methods of capacity expansion [6] of upstream power grid are less feasible due to high capital investment costs, land and resource restrictions, and long construction cycle [7]. Such power generation expansion schemes with additional power transmission and distribution capacity will eventually lead to higher electricity usage costs at airports. At the same time, power grid expansion will cause higher transmission losses and emissions from power industry [8]. ii) The purpose of the airport electrification is to reduce energy consumption, emissions and operation costs. If the electricity demand is completely supplied by the upstream grid, the source of emissions will be shifted from aviation to power industry.

The large area of the airport including airport terminal roof, car park and other open land space are ideal for the development of photovoltaic (PV) power generation, which can provide the clean and self-sufficient airport energy supply. For example, Beijing Daxing International Airport has installed significant amount of PV power generation, with an average annual power generation of 6.1 million kWh [9]. However, the intermittent and volatility of PV generation requires energy

storage to smooth the output profile [10], and the lifetime of battery storage system (BSS) is not long enough to support the whole project life cycle: the airport project lifecycle is generally 20-25 years, while the BSS lifetime is generally 8-15 years with a large replacement cost. In addition, the consumption of PV energy at airport remote stands requires large construction costs of mid-low-voltage (MLV) power distribution network, and is often restricted by the land space from airport planning perspective. Therefore, a flexible power supply such as ground power unit (GPU) for aircraft at remote stands is needed to enable the mobile power supply.

Hydrogen generated from green sources is considered as a feasible solution to decarbonize the future energy systems [11]. Hydrogen is in the form of water and hydrocarbons, and exhibits the highest heating value per mass of all chemical fuels. Hydrogen is also regenerative and environmentally friendly. The clean production of hydrogen is obtained through the electrolysis of water from renewable energy [12]. The hydrogen energy system (HES) mainly includes electrolyzer, hydrogen storage tank (HST), and fuel cell generation unit (FC) [13]. Compared with BSS, HES has a long service life which can cover the general airport project life cycle of 25 years, except for hydrogen fuel cell with assumed life of 5 years. More importantly, there is no loss of hydrogen storage, and hydrogen energy is easy to transport [14]. In the future, molecular energy transmission may be applied, which can avoid the grid expansion as well as the energy storage losses [15]. The integration of hydrogen energy into the future airport energy systems is considered as a viable development trend for airport energy supply and storage.

The main electric loads for airport electrification are the aircraft ground energy consumption and the charging of airport EVs. There are two types of aircraft loads: load at contact stands and load at remote stands. The aircraft load at remote stands is highly mobile, which is traditionally supplied by onboard APU of aircraft. However, the use of onboard APU will produce significant emissions and noise in an airport. Hydrogen fuel cell generation carried by ground mobile power vehicle (GPV) will provide flexible and mobile power supply for aircraft at remote stands to replace onboard APU.

Therefore, there are urgent requirements to assess the feasibility, role and value for the integration of new energy resources such as PV, hydrogen supply and energy storage systems for airport electrification. The feasible design and optimization of future airport energy system are essential for the economic operation of the airport towards a low-carbon sustainable aviation.

1.2 Literature review

Existing energy system research work is mostly focused on the optimal design of energy system with energy resource integration. For optimal and economic design, Yang Y et al proposed a mixed integer linear programming model to design a district scale distributed energy resource [16], and Quashie M proposed a bi-level formulation for a coupled microgrid power and reserve capacity planning problem [17]. On the other hand, environmental benefit is also considered in the design of the

energy system. For example, Patrizia S proposed a framework for design of smart multi energy systems considering environmental performance maximization [18], and Ma T et al proposed an optimal planning model to design multi energy system, which can obtain optimal structure configuration and energy management strategies [19]. With the decarbonization of fossil fuel-based energy system and enhanced multi-vector and multi-sector energy coupling technologies [15], new forms of energy sources are gradually integrated into traditional energy systems. Hydrogen presents an attractive option to decarbonize the present energy system. Lux B et al developed a supply curve of electricity-based hydrogen in a greenhouse gas emission-free European energy system in 2050 to evaluate the techno-economic hydrogen production potential and the impact of its utilization on the rest of the energy system [20]. Sgobbi A et al assessed the role of hydrogen in a future European energy system under two climate scenarios, current policy initiative and long-term decarbonization plan, and the results indicated that hydrogen could become a viable option in 2030 [11].

Regarding airport energy system planning, most of the existing research is based on the energy saving initiatives of airport terminal. For example, Cardona E, et al analyzed the typical energy demand of the airport and proposed feasible economic and technical standards for evaluating third-generation power plants [21]. Cardona E presented an in-depth analysis for the Malpensa airport to optimize the design and operation of airport energy system [22]. Zhang Y, et al designed an operation optimization strategy based on a heat storage system for a newly built airport terminal in Qingdao China to minimize the cost of the terminal [23]. In addition, a few scholars have also studied the energy consumption of aircraft outside the terminal building. Aircraft parked at the gate either use its APU or bridge mounted AC power supply units for maintaining cabin comfort, which is considered as an expensive and inefficient energy supply. Kılkıs B proposed a central air system connected to airport energy system, the Nearly-Zero Exergy Airport concept that brought an energy, environment, and economic nexus to a common basis using the second-law of thermodynamics [24]. Some researchers also investigated the benefits of such centralized systems [25] and demonstrated the airlines and airports may achieve an effective and efficient solution in close collaboration [26]. However, the centralized energy supply system is less flexible, which requires the installation of corresponding energy infrastructure, and has limited applications to the aircraft at remote stands. Therefore, aircraft in remote stands requires more flexible and sustainable energy supply.

Several studies have investigated the role and value of PV and energy storage integration to the airports. Chen CY et al analyzed the energy storage and power generation technologies with the application scenarios in Shanghai Pudong Airport [27]. Sreenath S et al analyzed the technical performance [28] and risks [29] of a proposed solar PV plant in Kuantan Airport, Malaysia. Yu JL analyzed the decarbonization potentials with the implementation of vehicle electrification in airport [30].

Silvester S et al took Amsterdam Airport Schiphol as an example to explore the feasible method for large-scale implementation of electric vehicles in airport [31]. Yang Y et al proposed an isolated optical storage system as an APU replacement, but the work only considered the replacement of APU at remote stands [32]. In addition, there are actually PV energy integration in airports such as Beijing Daxing International Airport [9], Chattanooga Metropolitan Airport [33], and Copenhagen Airport [34]. These real-world case studies have shown the benefits of the airport's energy access from PV and energy storage as the necessary part of airport electrification program.

The research on hydrogen energy system (HES) mainly focuses on the supply, storage and usage of hydrogen energy. For example, Apostolou D explored the implementation of hydrogen technologies in the electricity network as a power generation unit and utilized the hydrogen as a transportation fuel in Denmark [35]. Seo SK, et al proposed a hydrogen supply chain optimization model using a centralized storage model that combines and consolidates flows of hydrogen from different production sites into the integrated bulk storage [36]. The result showed the centralized hydrogen storages can effectively reduce the cost comparing with the decentralized model. AINouss A, et al proposed a biomass gasification process with subsequent optimization by considering multiple parameters, which includes the feedstock and agent(gasifier) to maximize hydrogen production [37]. Farahani S, et al presented the concept design and energy management of an integrated energy and mobility system in real-life environment at the Shell Technology Centre in Amsterdam [38]. The result of this study showed that the utilization of both electricity and hydrogen as energy carriers can create a more flexible, reliable and cheaper energy system at an office building. In addition, Wu X, et al proposed an optimal scheduling model for microgrids with hydrogen fueling stations by considering wide range of uncertainties from renewable generation, electrical and hydrogen loads, and electricity price [39]. Qiu Y, et al explored the feasibility of underground hydrogen storage facilities in the integrated energy system in China as case studies [40]. The above studies on HES have shown the benefits of integrating HES into different energy system applications and scenarios. However, the integration of HES to the airport energy system has not been fully developed, with limited application such as hydrogen-powered ground support vehicles in airport [41].

1.3 Contributions

This paper innovatively introduces hydrogen-solar-storage integrated microgrid system for airport electrification. The energy system of airport outside the terminal is designed as a direct current (DC) microgrid system. The aircraft APU and EVs in the airport are integrated into the DC microgrid. The integration of HES has established an energy link between the DC microgrid system and the aircraft energy supply at remote stands. More specifically, the GPV equipped with hydrogen fuel cells provide sufficient flexibility and mobility for the power supply of aircraft in the airport, while avoiding the

infrastructure investments on mid-low-voltage power distribution networks in future airports.

The main contributions of this paper are summarized as follows:

- This paper innovatively introduces the hydrogen, solar, and energy storage into the future airport as a microgrid energy system. A mixed integer linear programming (MILP) optimization method based on lifetime cycle theory is developed to design the capacity of each energy sources, which aims at minimizing the total costs under the life cycle of airport project, and assessing the economic and environmental benefits of the hydrogen-solar-storage integrated microgrid for airport electrification.
- Based on the flight schedules, an airport APU load characteristic model is established to quantify aircraft ground power requirements. A method for generating EVs charging profile in airport based on flight schedule and sequencing algorithm is proposed.
- Five different scenarios are studied and compared to assess the economic and environmental benefits of hydrogen-solar-storage integrated microgrid for future airport design and operation. The sensitivity analysis of key parameters such as solar irradiance, carbon tax, HES investment costs and electricity price that impact the costs and revenue of the proposed airport energy system have been investigated.

The paper is structured as follows: Section 2 describes the architecture of energy system in airport; In Section 3, the modelling approach and methodology for airport energy system are presented; Section 4 proposes the optimization method for airport energy system design and operation; Case studies with five energy integration scenarios are illustrated in Section 5; Results and discussion are conducted in Section 6; Conclusions are drawn in Section 7.

2. ARCHITECTURE OF AIRPORT ENERGY SYSTEM

2.1 General structure of airport

An airport is generally composed of the following parts [42]: 1) Flight area, including runways, taxiways, and liaison roads; 2) Parking apron; 3) Terminal; 4) Navigation tower; 5) Auxiliary parts of the airport, including aircraft maintenance garage, fueling system, etc. This article is mainly focused on the optimal design and operation of energy system outside the terminal. The energy supply targets are mainly aircraft and EVs. A schematic airport diagram is shown in Fig. 1. Generally, passengers will be arranged with different boarding methods dependent on the location of the aircraft. Passengers of the aircraft parked in contact stands can board the plane through the boarding bridge, while aircraft parked in remote stands need to take the shuttle bus to the aircraft dock to board the plane. It is assumed that there is a power supply installed under each boarding bridge at contact stands to supply power for the aircraft (aircraft power standard is: 115V /200V, 400Hz) [43].

Some airports have power distribution boxes at apron, which needs to be connected to the power car through a long-distance intermediate power cable [44]. The mains power of 400Hz installed in power car is used to convert the power frequency to meet the power requirements of the aircraft at remote stands [44]. However, majority of airports still use onboard APU to supply aircraft at remote stands. In addition, electric vehicles at the airport are increasingly used to replace traditional fuel vehicles.

The energy consumption outside terminal building mainly includes ground power supply for the aircraft to replace the aircraft APU and EVs charging. Such energy demand will be supplied by a multi-energy system design including PV, BSS, HES, and DC microgrid.

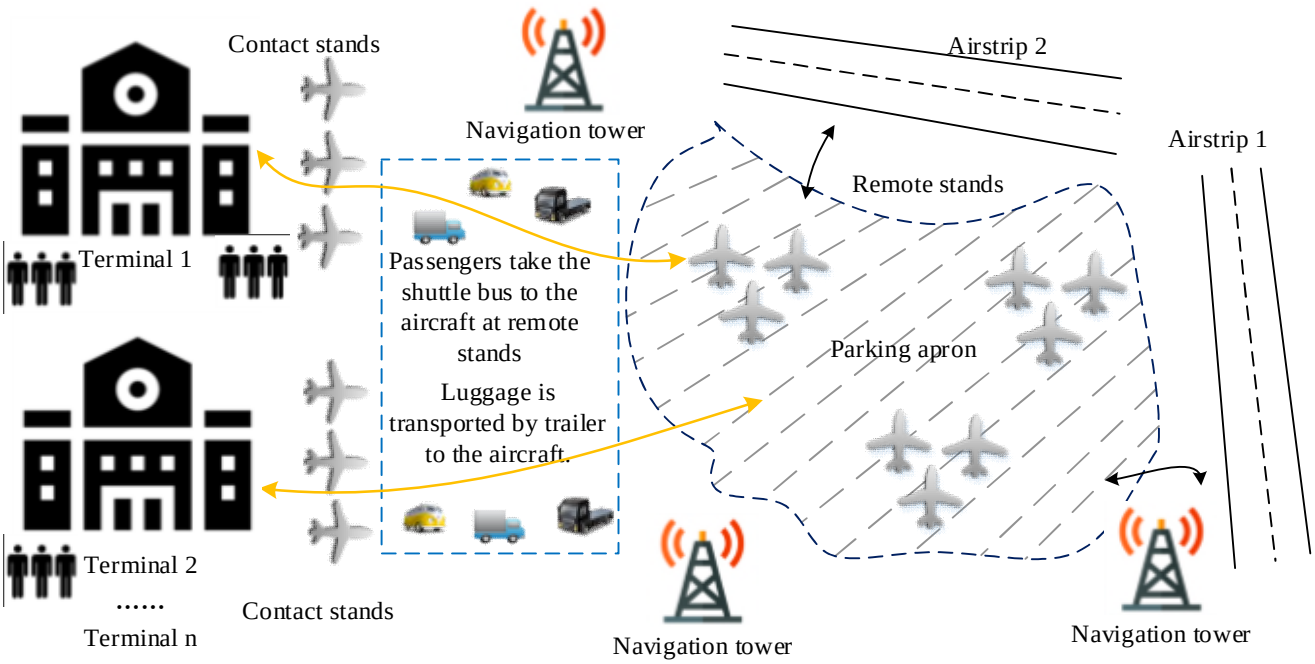

Fig. 1 General structure of airport with airside and landside areas.

2.2 Energy supply and demand for airport electrification

To improve the energy supply and reduce carbon emissions for airport electrification, the new energy sources are integrated in airport. Solar energy is the main renewable energy considered for airport energy system, where the PV can be installed on the roof of the terminal and open space in the apron. The PV energy is used to supply aircraft electric APU and EVs demand. Due to the supply demand imbalance of PV generation, BSS is planned to store the excess PV in the form of electricity. In addition, HES is innovatively used in airport environment to store the excess PV energy through power-to-gas, where the excess PV energy is transformed to hydrogen and oxygen using electrolyzer. The produced green hydrogen is stored in HST can be used to supply airport load at remote stands through fuel cell generator as a mobile distributed generation. The produced

oxygen can be sold as industrial oxygen or medical oxygen to provide extra revenue for airport energy operation. All the distributed energy supply and demand are connected and managed together via a microgrid system by an energy control center. The overall energy supply and demand diagram of future airport is presented in Fig. 2. In the section 3, the detailed energy system modelling is presented.

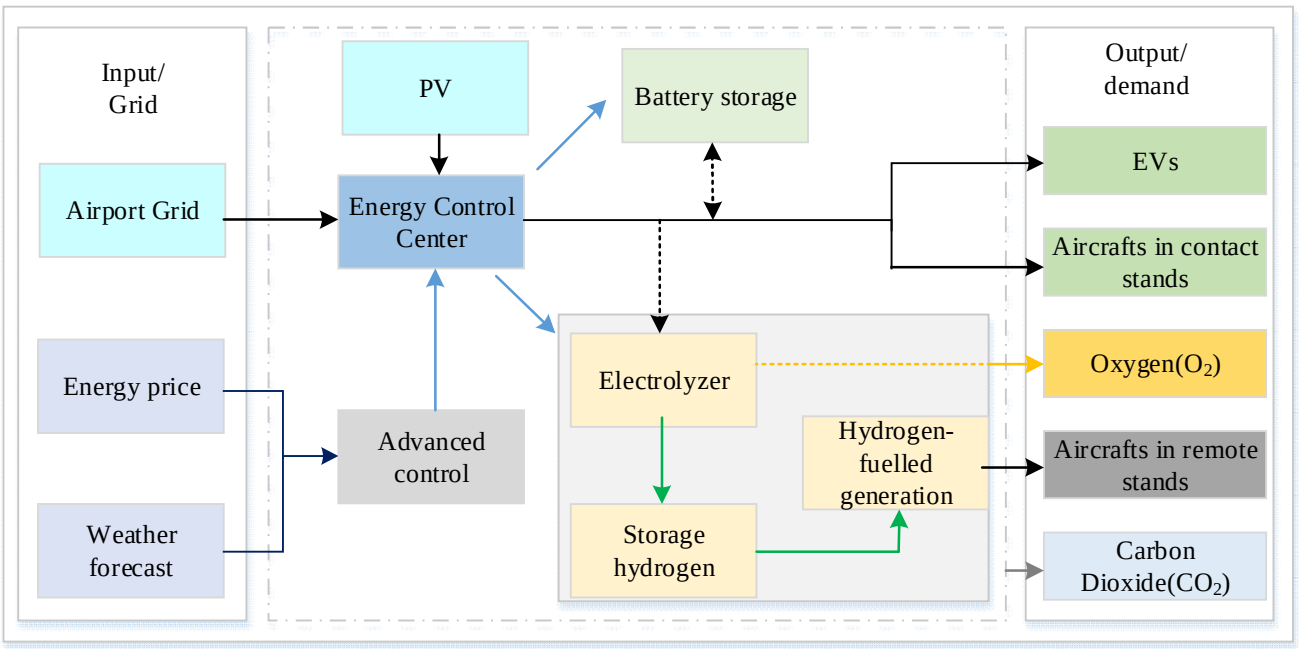

Fig. 2 Energy supply and demand for airport electrification

2.3 DC microgrid energy system for airport

DC microgrid energy system is proposed for future airport to integrate multiple DC energy supplies including PV, batteries, EVs, and hydrogen electrolyzer. For traditional AC power grid, inverters are usually needed to convert the power generation or storage from DC into AC that can be delivered through an AC power distribution system. The DC/AC energy conversion at both supply and demand sides not only causes electricity losses, but also reduces the system reliability due to the power conversion complexity [45]. The structure of the DC microgrid aims to minimise the convertor architecture with high quality of power supply and eliminate reactive power and phase imbalance issues [46]. Therefore, a new energy supply structure based on DC microgrid is proposed to replace the traditional AC distribution system in future airport [47].

Fig. 3 presents the schematic design of DC microgrid for future airport electrification. This system integrates multiple energy sources with different energy carriers through convertors, energy distribution and storage components in an optimal manner for various airport energy use. The FC in the HES is not directly connected to the DC microgrid. Instead, the fuel cell generator is installed on the ground vehicle and designed as mobile power source, which are used to supply electricity

for aircraft at remote stands. The electrolyzer connected to the DC microgrid with attached HST provide green hydrogen production and storage on-site. The different nodes in the microgrid, such as PV, FC, HES, BSS, EVs and electric loads, can exchange power by autonomous distributed control systems based on the DC voltage. The energy control center automatically controls all the system components to ensure optimal energy dispatch and utilization within the DC grid. The operation voltage of the DC microgrid is designed to be 600V, which can directly interface with battery storage system (BSS) in this study. The 600V DC grid voltage is then stepped down to the output voltage required by loads (380V/400V).

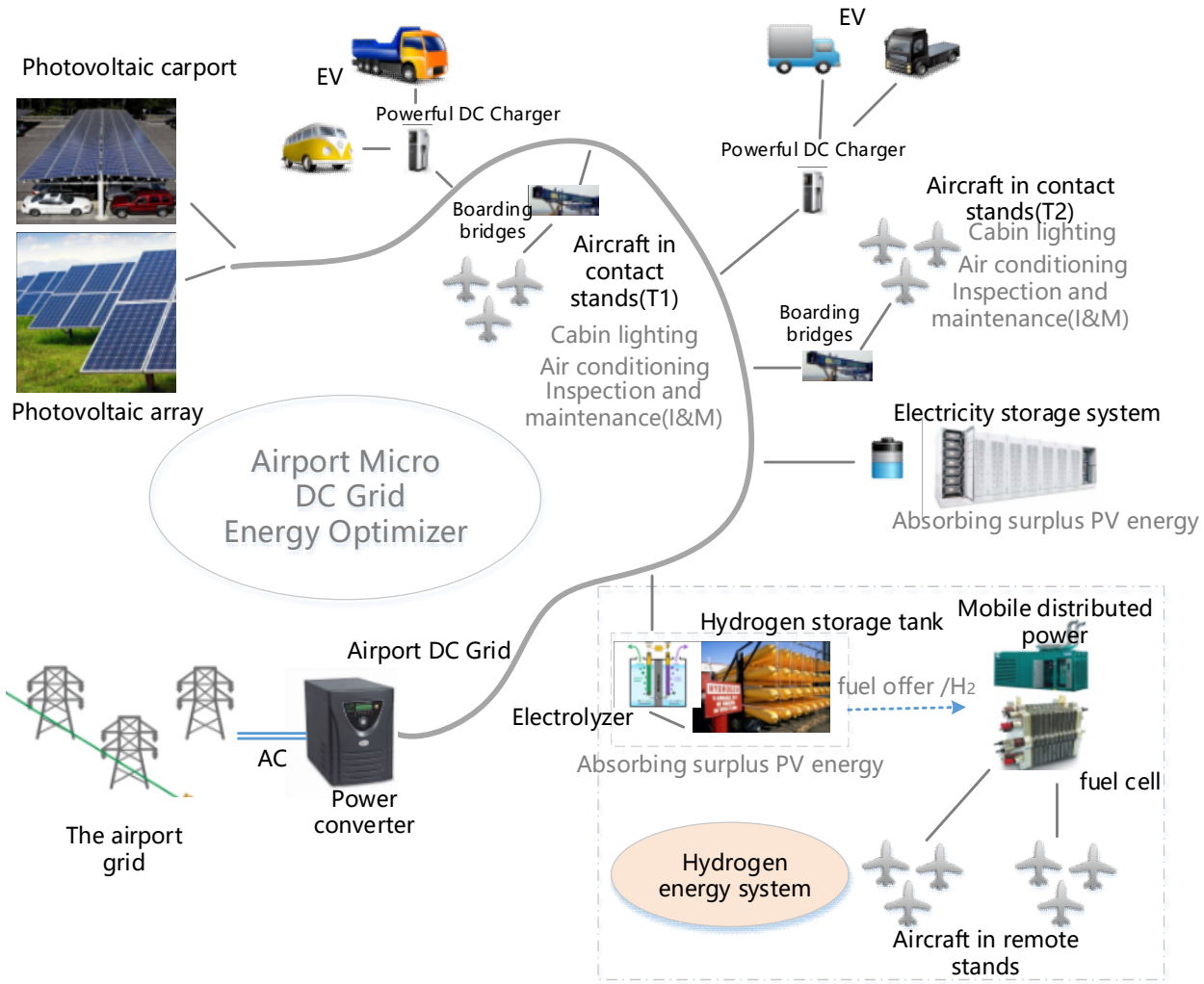

Fig. 3 Schematics of the airport energy supply structure based on DC microgrid

3 MODELLING APPORACH FOR AIRPORT ENERGY SYSTEM

3.1 Photovoltaic system modelling

The large area of the airport provides sufficient land availability for photovoltaic (PV) power plants. The layout of PV power plants can be designed as photovoltaic carports (The parking lot is designed with photovoltaic carports to reduce the

floor space) in addition to rooftop photovoltaic and open space in airport. The PV panel uses monocrystalline silicon solar panels (250W) with length and width of 1.64m and 0.99m, respectively. The unit capacity of PV is 1kW, which is composed of four 250W PV panels. The power output of PV panels can be expressed as follows [48]:

$$P_{t,pv}^{out} = N_{pv} P_{STC} \frac{I_t}{I_{STC}} [1 + \alpha (T_{t,c} - T_{c,STC})] \quad (1)$$

where $P_{t,pv}^{out}$ is the output power of PV at time slot *t*, N_{pv} is the number of PV panels, and P_{STC} is the rated power of PV panel at standard text conditions(STC, Cell temperature 25℃, irradiance 1000W/m^2), I_t is the solar radiation intensity at time slot *t*, I_{STC} is the irradiance intensity at STC, α is the temperature coefficient of power, $T_{t,c}$ is the PV cell temperature at time slot *t*, $T_{c,STC}$ is the PV cell temperature under STC.

3.2 Battery storage system modelling

The battery energy storage system (BSS) is used for the storage of excess photovoltaic energy. In a microgrid system, a BSS can be considered as a load when it charges, conversely, it can be treated as a generation source when it discharges. Li-ion batteries have high energy density, low self-discharge, fast charging, and good safety performance [49]. Therefore, Li-ion batteries are applied to battery storage systems in this study, which consists of multiple energy storage units. The bus voltage of the energy storage system is designed to be 600V, which consists of 100 1kWh/6V lithium batteries connected in series. The battery storage model can be formulated as follows [50]:

$$E_{t+1}^{BSS} = (1-\delta) E_t^{BSS} + (\eta^c P_t^{in,BSS} - P_t^{out,BSS} / \eta^d) \Delta t \quad (2)$$

where E_{t+1}^{BSS} and E_t^{BSS} denote the energy stored at time slots *t*+1 and *t*, δ is the standby energy loss ratio, η^c and η^d are the charging efficiency and discharging efficiency. $P_t^{in,BSS}$ and $P_t^{out,BSS}$ denote the charging and discharging power. Δt is the time step.

3.3 Hydrogen energy system modelling

Hydrogen energy system (HES) can provide a low-carbon sustainable power source for renewable energy system. Hydrogen fuel cell is pollution-free, noise-free, and highly efficient [51]. The fuel cell power generation is designed by combining multiple small fuel cell units as a whole that can meet the maximum load at remote stands.

An electrolyzer with low-temperature category is used as a suitable application in the airport environment, and have the ability to deliver 99.99% pure, dry, carbon-free and pressurized hydrogen without a compressor [52]. These features can be coupled with solar energy for on-site hydrogen production. The Proton exchange membrane (PEM) fuel cell is selected in

this study due to its characteristics of reliable operation. The operating temperature of PEM is low (about 80 °C) with a short start-up time and can reach full load in a few minutes. The power generation efficiency is relatively high (45% -60%). An electrolyzer is used to produce hydrogen and oxygen, and the fuel cell reverses the process from gas to power. The electrolyzer and fuel cell are modelled in Eq. (3)[53] and Eq. (4)[54], respectively:

$$m_t^{out,H_2} = \frac{3.6 P_t^{in,electrolyzer} \Delta t}{h_{\mathrm{HHV}}^{H_2}} \eta^{electrolyzer}$$
$$m_t^{out,O_2} = 8 m_t^{out,H_2} \tag{3}$$

$$P_t^{FC} = a + b F_t^{H_2} \tag{4}$$

where m_t^{out,H_2} denote the amount of hydrogen produced by electrolyzer at time slot *t* (kg/hr), $P_t^{in,electrolyzer}$ is the power input to the electrolyzer, $h_{\mathrm{HHV}}^{H_2}$ is the higher heating value of hydrogen (MJ/kg), $\eta^{electrolyzer}$ is the efficiency with which the electrolyzer converts electricity into hydrogen, m_t^{out,O_2} is the amount of oxygen produced by electrolyzer at time slot *t*. $F_t^{H_2}$ is the hydrogen consumption rate(kg/hr), P_t^{FC} is the output of fuel cell at time slot *t*, *a* and *b* are power generation coefficients of fuel cell.

The low temperature liquid hydrogen storage tank (HST) is used as a storage medium between the electrolyzer and the mobile fuel cell unit that supply the aircraft at remote stands. The HST model can be formulated as follows [53]:

$$m_{t+1,H_2}^s = m_{t,H_2}^s + \left(m_{t,H_2}^{s,in} - m_{t,H_2}^{s,\mathrm{out}} \right) \Delta t \tag{5}$$

where $m_{t,H_2}^{s,in}$ and $m_{t,H_2}^{s,\mathrm{out}}$ denote the hydrogen charging/discharging flow (kg/hr), m_{t+1,H_2}^s and m_{t,H_2}^s denote hydrogen stored at time slots *t*+1 and *t*.

3.4 Aircraft electric load modelling

To replace aircraft fuel-based APU for electrification, the aircraft needs to be powered by airport ground power source during turnaround time to carry out the flight preparation work and provide a comfortable cabin environment for passengers. Based on the flight schedule [55] shown in Fig. 4, an hourly-based aircraft APU load characteristic model is established to obtain new electric load profile of aircraft. The flight schedule is derived from a case study airport (in Section 5) in Chengdu China, but the load modelling method can be used for other airports to estimate electric load of aircraft.

Flight No.	From	To	Via	Departure Time	Terminal	Status
YG9028	CHENGDU	XI' AN		04:20	T2	Take Off At 04:29
3U3713	CHENGDU	BRUXELLES		04:35	T1	Take Off At 06:33
CX2061	CHENGDU	HONGKONG		04:45	T2	Take Off At 05:12
CA403	CHENGDU	SINGAPORE CHANGI		05:00	T2	Take Off At 05:18
UA2802	CHENGDU	TOKYO NARITA		05:15	T2	Take Off At 05:07
3U8225	CHENGDU	BRUXELLES		05:40	T1	Take Off At 06:00
Y87938	CHENGDU	SHANGHAI PUDONG		05:50	T2	Take Off At 06:19
GJ8686	CHENGDU	HANGZHOU		05:55	T2	Take Off At 06:05

(a) Flight departure

Flight No.	From	To	Via	Arrival Time	Terminal	Status
MU2230	HEFEI	CHENGDU		00:05	T2	Arrive At 23:19
3U8814	DALIAN	CHENGDU		00:20	T1	Arrive At 23:55
MU4050	DALIAN	CHENGDU		00:20	T1	Arrive At 23:55
3U8570	DUNHUANG	CHENGDU		00:20	T1	Arrive At 23:46
EU2240	FUZHOU	CHENGDU		00:25	T2	Arrive At 23:50
HO3475	FUZHOU	CHENGDU		00:25	T2	Arrive At 23:50
CA4238	ZHANJIANG	CHENGDU		00:25	T2	Arrive At 00:01

(b) Flight arrival

Fig. 4 Part of flight schedule for aircraft electric load modelling

Some assumptions are made to simplify the aircraft electric load modelling: i) The aircraft taxiing time from the terminal to airstrip is not counted, as it is considered that the aircraft is powered by its main engine for departure; ii) The APU replacement power of all aircraft is assumed to be the same regardless of aircraft type; iii) The aircraft will have priority to park at contact stands where possible, when the contact stands are full, the aircraft will be directed to remote stands.

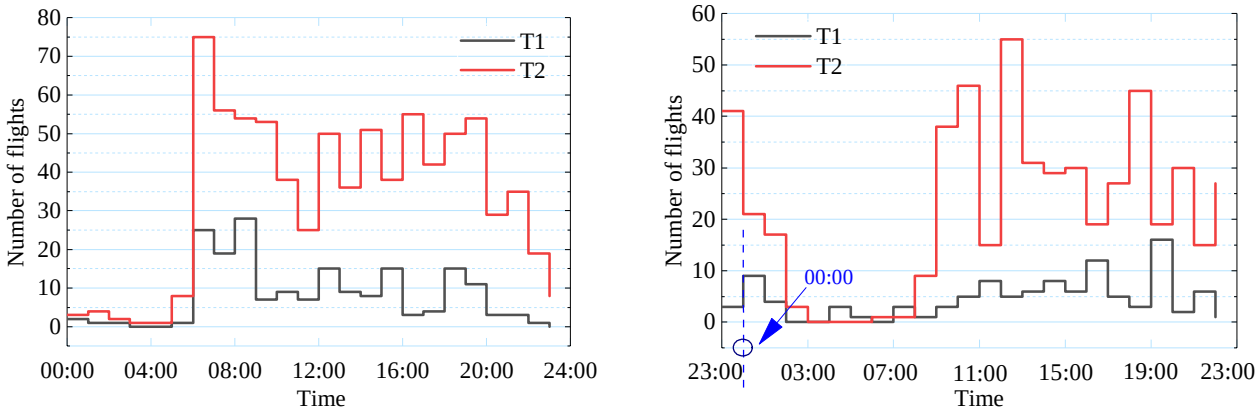

(a) Departure (b) Arrival

Fig. 5 Number of flights arrival and departure on a typical day

The departure / arrival flow curves from different terminals on a typical day are obtained based on flight schedule as shown in Fig. 5. The electric load for aircraft at contact stands and remote stands can be calculated by the Eq. (6) and Eq. (7) respectively. The load profile of aircraft on a typical day is shown in Fig. 6.

$$P_{t,conract\ stands}^{aircrafts} = P_{AVE}^{aircraft}\left\{\begin{array}{l}\min[\int_{t}^{t+t^{dep}} D_{Aircraft}^{depature,T1}(t)dt + \int_{t-t^{arr}}^{t} D_{Aircraft}^{arrival,T1}(t)dt, B^{T1}] \\ +\min[\int_{t}^{t+t^{dep}} D_{Aircraft}^{depature,T2}(t)dt + \int_{t-t^{arr}}^{t} D_{Aircraft}^{arrival,T2}(t)dt, B^{T2}]\end{array}\right\} \tag{6}$$

$$P_{t,remote\ stands}^{aircrafts} = P_{AVE}^{aircraft}\left\{\begin{array}{l}\max[\int_{t}^{t+t^{dep}} D_{Aircraft}^{depature,T1}(t)dt + \int_{t-t^{arr}}^{t} D_{Aircraft}^{arrival,T1}(t)dt - B^{T1}, 0] \\ +\max[\int_{t}^{t+t^{dep}} D_{Aircraft}^{depature,T2}(t)dt + \int_{t-t^{arr}}^{t} D_{Aircraft}^{arrival,T2}(t)dt - B^{T2}, 0]\end{array}\right\} \tag{7}$$

where $P_{t,conract\ stands}^{aircrafts}$ and $P_{t,remote\ stands}^{aircrafts}$ are the load demand of aircraft at contact and remote stands at time slot *t*, respectively. $P_{AVE}^{aircraft}$ represents the average electrical power demand of aircraft, $D_{Aircraft}^{depature,T1}(t) / D_{Aircraft}^{arrival,T1}(t)$ denote the departure/arrival flow curve function of terminal 1(T1), and $D_{Aircraft}^{arrival,T1}(t) / D_{Aircraft}^{arrival,T2}$ denote the departure/arrival flow curve function of terminal 2(T2). B^{T1} / B^{T2} indicate the number of contact stands (boarding bridges) of T1 and T2. t^{dep} is the time preparing for flighting before departure, and t^{arr} is the time of passengers disembarking, cleaning and maintenance after arrival.

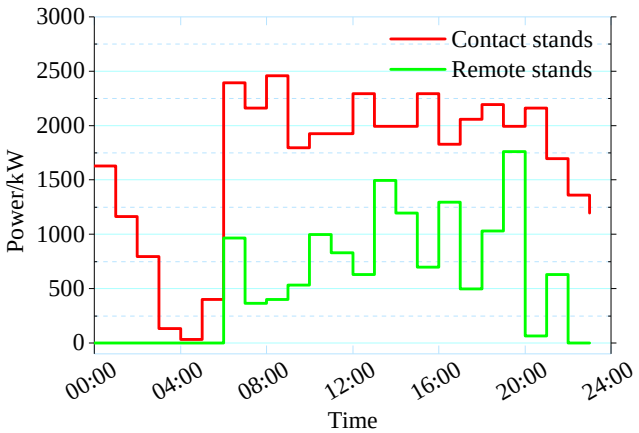

Fig. 6 Aircraft hourly electric load profile at contact and remote stands

3.5 Electric vehicle charging load in airport

The airport has a set of electrified ground support vehicle in airside for passengers and goods transportation. The novelty of this research work is to integrate flight schedules into the operation of EVs in airport. A method for generating EVs charging profile in airport based on flight schedules and sequencing algorithm is proposed in Fig. 7. Each EV in airport has a number of variables in the "vehicle matrix" which includes the EVs' state of charge (SOC), availability, current state and tag number [56]. The SOC is initially set randomly by a random uniform distribution. EV availability λ_{EV}, affected by SOC and current state, is the available number of EVs with SOC greater than SOC_{min} at each time slot. EV current state is used to indicate whether the electric vehicle is charging. The number of flights coming in at the given time slot determines how many of EVs are required. The required number for EVs at time slot *t*, denoted as $D_{EV}(t)$, is equal to the number of flights in the current time slot multiplying by the average number of service vehicles required for an aircraft. For every time slot, each EV is ranked and updated according to the attributions within the vehicle matrix. EVs with lower SOC will have higher rank and thus have charging priority over other EVs. EVs with higher SOC will have dispatch priority to serve aircraft.

When there are insufficient EVs at a time step to cover the required aircraft ground service, gas vehicles are used to fill

the shortage. The number of EVs that can be charged at any time is mainly determined by the number of charging piles (N_{CP}) and EVs that have not been dispatched ($N_{udp}(t)$). Then, the SOC of each EV is updated at each time slot *t*. If the EV is charging, the SOC increases by the charging rate during the time step (Eq. (8)). Conversely, the SOC decreases by the EV energy consumption rate to service an aircraft (Eq. (9)). The objective of EV dispatch algorithm is to maximize the numbers of EV usage for the whole period of 24 hours.

$$SOC_t^{final} = SOC_t^{initial} + SOC_t^{charge} \tag{8}$$

$$SOC_t^{final} = SOC_t^{initial} - SOC_t^{service} \tag{9}$$

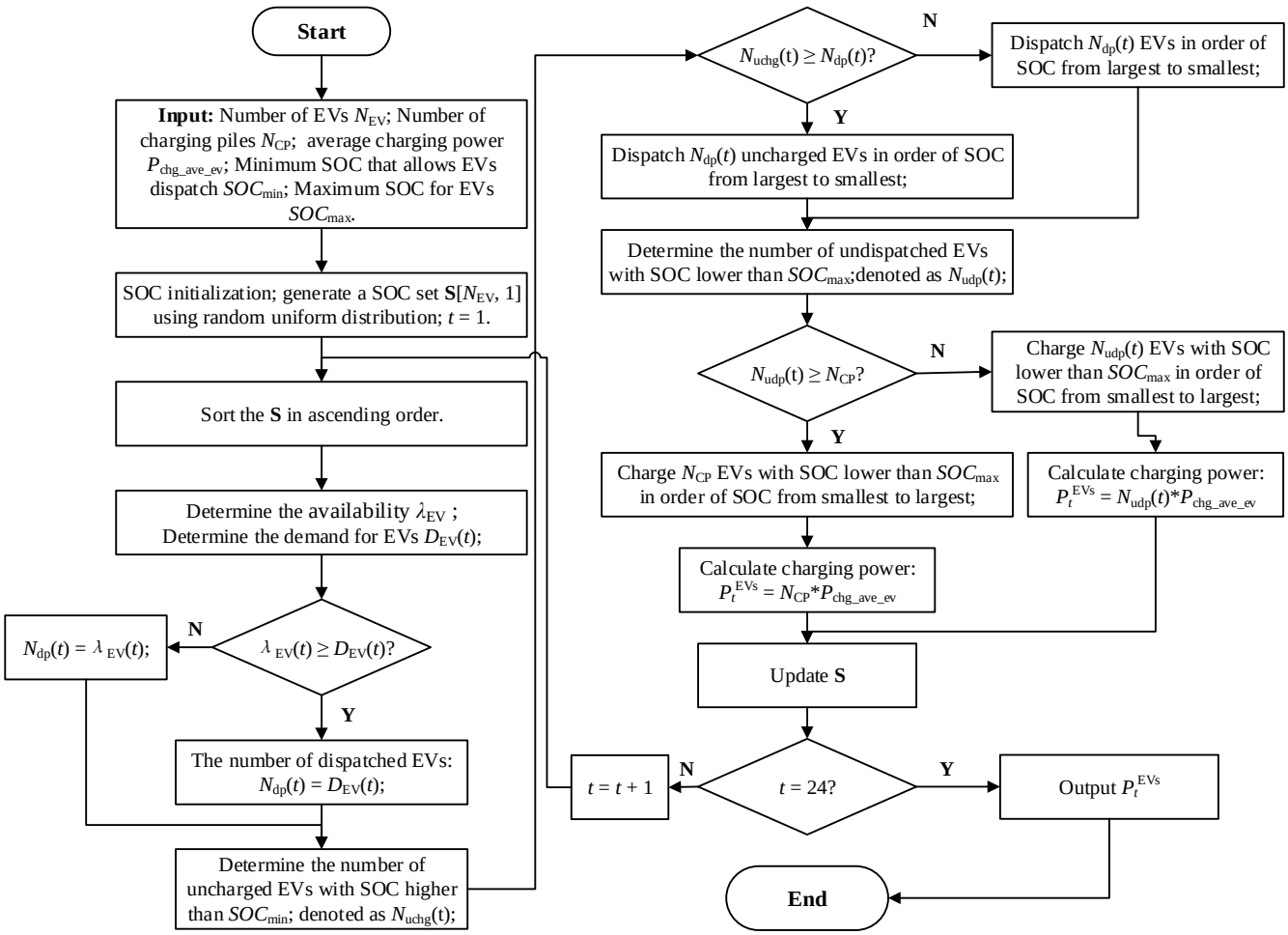

Fig. 7 Flow chart of EVs charging profile modelling

Fig. 8 shows the modelling results of hourly EVs charging load profile on a typical day. The charging load is almost zero during 05:00-09:00 due to the less flights are scheduled at 05:00 (All EVs are fully charged), and the initial flight peak period is at 06:00-09:00 (All EVs are dispatched).

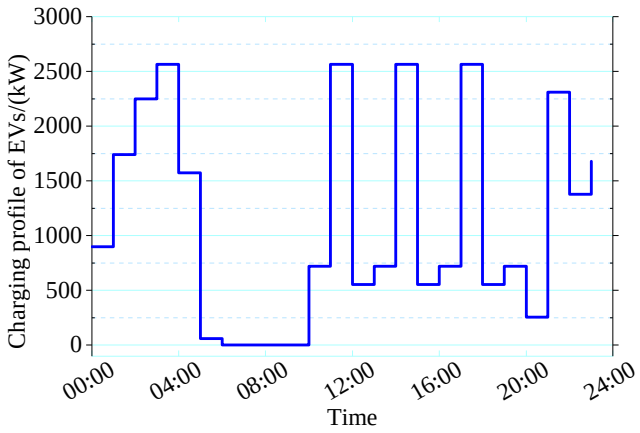

Fig. 8 Charging load profile of EVs in airport

4. OPTIMIZATION OF AIRPORT MICROGRID ENERGY SYSTEM

The airport microgrid energy system model is formulated by a mixed integer linear programming (MILP) method with an annually time horizon and hourly time resolution. The model consists of investment, operation and emission costs of airport microgrid energy system as shown in Eq. (10).

4.1 Objective function

The objective function shown in Eq. (10) is to minimize the overall investment, operation and emission costs of airport microgrid energy system. The objective function is formulated as follows:

$$Min\ \varphi = \frac{j(1+j)^N}{(1+j)^N - 1} \sum_{y=0}^{N} \frac{C_y^{inv}}{(1+j)^y} + C^{op} + C^{CO_2} \tag{10}$$

$$C_y^{inv} = \sum_{i \in \Omega^{device}} \begin{bmatrix} \pi_i^{inv} \psi_i^{cap} (y=0) + \pi_i^{rep} \psi_i^{cap} (device\ i\ is\ replaced\ in\ year\ y) \\ -\pi_i^{rep} \psi_i^{cap} \frac{l_i^{rem}}{l_i^{comp}} (y=N) \end{bmatrix} \tag{11}$$

$$\begin{aligned} C^{op} = & \sum_{t=1}^{T} \pi_t^{electricity\ price} P_t^{grid,buy} \Delta t + \sum_{m=1}^{12} \pi^{demand} P_{month}^{demand,\max} + \sum_{i \in \Omega^{device}} \pi_i^{O\&M} \psi_i^{cap} \\ & + \sum_{t=1}^{T} \pi^{unmet,H_2} m_t^{unmet,H_2} - \sum_{t=1}^{T} \pi^{Oxygen\ price} m_t^{out,O_2} \Delta t \end{aligned} \tag{12}$$

$$C^{CO_2} = \pi^{CO_2} \sum_{t=1}^{T} d_{grid}^{CO_2} P_t^{grid,buy} \Delta t \tag{13}$$

where,

- C_y^{inv} represents the investment cost incurred in year *y*, which includes the initial investment in year 0, the replacement cost of equipment during the project cycle and the salvage value of equipment at the end of the project cycle.
- C^{op} denotes the annual operating cost, which includes the purchase cost of electricity, equipment operation and maintenance(O&M) cost, penalty cost of unmet hydrogen, and revenue from the sale of oxygen.
- C^{CO_2} is the annual carbon dioxide (CO_2) emission cost derived from power grid.
- $j$is the discount rate, N is the project lifecycle, Ω^{device} is the device set, π_i^{inv} denotes the unit investment cost of equipment i, ψ_i^{cap} is the capacity of device i(kW, kWh), π_i^{rep} denotes the unit replacement cost of equipment i, l_i^{comp} is the lifetime of device i, and l_i^{rem} is the remaining lifetime of device i at the end of the project cycle; T is the total number of time slots in one year, $\pi_t^{electricity\ price}$ is the electricity price at time slot t (\$/kWh), $P_t^{grid,buy}$ is the power purchased from grid at time slot t(kW), $P_{month}^{demand,\max}$ denotes the maximum power demand per month(kW), π^{demand} is power demand charge(\$/kW), $\pi_i^{O\&M}$ is the unit O&M cost of equipment i(\$/kW), π^{unmet,H_2} denotes penalty cost of hydrogen shortfall (\$/kg), m_t^{unmet,H_2} is the unmet hydrogen in time slot t, $\pi^{Oxygen\ price}$ is the price of oxygen, π^{CO_2} is the carbon tax (\$/kg), $d_{grid}^{CO_2}$ denotes the grid emission factor (kg/kWh).

4.2 Constraints

The proposed airport microgrid energy system models are subject to planning and operation constraints. All constraints are applied to each time interval within the optimisation time horizon. Electricity supply and demand are balanced in each time interval (Eq. (14)). Hydrogen supply from fuel cell power generation to aircraft at remote stands should be guaranteed (15). The installed capacity of the equipment is subject to geographical conditions and other relevant factors (Eq. (16)). The power output of each energy sources including PV, hydrogen electrolyser and fuel cell must remain within the maximum operation range following by the safety and reliability requirements of each energy system (Eq. (17)). The constraints of energy storage systems including BSS and HST are expressed in Eq. (18) and Eq. (19), respectively.

$$\begin{aligned} P_t^{grid,buy} + P_t^{pv} + P_t^{out,BSS} - P_t^{in,BSS} &= P_{t,contact\ stands}^{aircrafts} + P_t^{EVs} + P_t^{in,electrolyzer} \\ P_t^{FC} &= P_{t,remote\ stands}^{aircraft} \\ F_t^{H_2} - m_t^{unmet,H_2} &= m_t^{out,H_2} + m_{t,H_2}^{s,out} - m_{t,H_2}^{s,in} \end{aligned} \tag{14}$$

$$\begin{aligned} \sum_{t=1}^{T} m_t^{unmet,H_2} &\le \lambda^{unmet,H_2} \sum_{t=1}^{T} F_t^{H_2} \\ 0 \le m_t^{unmet,H_2} &\le F_t^{H_2} \end{aligned} \tag{15}$$

$$\varphi_i^{cap,\min} \le \varphi_i^{cap} \le \varphi_i^{cap,\max} \tag{16}$$

$$\begin{cases} 0 \le P_t^{pv} \le P_{t,pv}^{out} \\ P_{\min}^{in,electrolyzer} \le P_t^{in,electrolyzer} \le P_{\max}^{in,electrolyzer} \\ P_{\min}^{FC} \le P_t^{FC} \le P_{\max}^{FC} \end{cases} \tag{17}$$

$$\begin{cases} 0 \le P_t^{in,BSS} \le u(\mathrm{t}) P_{\max}^{in,BSS} \\ 0 \le P_t^{out,BSS} \le (1-u(\mathrm{t})) P_{\max}^{out,BSS} \\ E^{\min} \le E_t^{BSS} \le E^{\max} \end{cases} \tag{18}$$

$$\begin{cases} v(t) m_{\min,H_2}^{s,in} \le m_{t,H_2}^{s,in} \le v(t) m_{\max,H_2}^{s,in} \\ (1-v(t)) m_{\min,H_2}^{s,\mathrm{out}} \le m_{t,H_2}^{s,\mathrm{out}} \le (1-v(t)) m_{\max,H_2}^{s,\mathrm{out}} \\ m_{\min,H_2}^{s} \le m_{t,H_2}^{s} \le m_{\max,H_2}^{s} \end{cases} \tag{19}$$

where P_t^{pv} is the power consumed of PV at time slot t; P_t^{EVs} is the load of EVs at time slot t, $m_{t,H_2}^{s,in}$ and $m_{t,H_2}^{s,\mathrm{out}}$ denote the hydrogen charging/discharging flow (kg/hr); λ^{unmet,H_2} is the proportion of unmet hydrogen; $\varphi_i^{cap,\min}$ and $\varphi_i^{cap,\max}$ are the upper and lower limits of φ_i^{cap}, $P_{\min}^{in,electrolyzer}$ and $P_{\max}^{in,electrolyzer}$ are the upper and lower limits of $P_t^{in,electrolyzer}$, $P_{\min}^{FC}$ and $P_{\max}^{FC}$ are the upper and lower limits of fuel cell generation; $P_{\max}^{in,BSS}$ and $P_{\max}^{out,BSS}$ are the maximum charging and discharging power of BSS, $E^{\min}$ and $E^{\max}$ are the upper and lower limits of BSS's capacity; $m_{\min,H_2}^{s,in}$ and $m_{\max,H_2}^{s,in}$ are the upper and lower limits of $m_{t,H_2}^{s,in}$, respectively. $m_{\min,H_2}^{s,\mathrm{out}}$ and $m_{\max,H_2}^{s,\mathrm{out}}$ are the upper and lower limits of $m_{t,H_2}^{s,\mathrm{out}}$ respectively. m_{t+1,H_2}^{s} and m_{t,H_2}^{s} denote hydrogen stored at time slots t+1 and t. $m_{\min,H_2}^{s}$ and $m_{\max,H_2}^{s}$ are the upper and lower limits of stored hydrogen. $u(\mathrm{t})$ and $v(t)$ are auxiliary binary variables for BSS and HTS to respectively constrain that the charging and discharging processes will not occur simultaneously.

5. CASE STUDY

Based on the general airport structure and optimization model established above, case study is conducted for techno-economic and environmental analysis of the proposed airport microgrid energy system with five energy supply scenarios.

5.1 Input parameters

The case study requests a series of input parameters including environmental, technical and economic parameters. The environmental inputs are mainly local weather and geographic information such as airport roof and open space area. The average ambient temperature and annual solar irradiance are 13.33℃ and 0.146kW/m^2, respectively.

The directly connected electric demand in the airport microgrid are aircraft (APU replacement) at contact stands and

EVs. The indirect electric demand is the aircraft (APU replacement) at remote stands. The aircraft hourly electric load profiles and EVs hourly charging load profile have been given in the section 3. In Fig. 9, the annual electric demand profile of airport energy system is estimated by monthly electricity demand, and the difference between months is mainly determined by flight schedules and weather conditions (temperature, etc.).

The economic inputs mainly include the capital investment, replacement and maintenance costs of each energy devices as summarized in Table 1. The project life cycle, discount rate, and carbon tax are 25years, 6%, and 20$/ton, respectively. The carbon emission factor, electricity price, aviation fuel price and oxygen price are shown in Table 2.

Table 1 Economic costs of energy devices [57, 58]

Devices	Capital cost	Replacement cost	Maintenance cost($/year)	Life time(years)
PV	574$/kW	-	8.43 $/kW	25
BSS	104.32$/kWh	96.87$/kWh	5.22$/kWh	10
Electrolyzer	632.79$/kW	-	66$/kW	25
Fuel cell	501.64$/kW	451.47$/kW	11.57$/kW	5
Hydrogen tank	1341$/kW	-	15.65$/kg	25

Table 2 Energy prices and emission cost [59, 60]

Items	Time interval	Value
Electricity price	23:00-6:00	0.0835$/kWh
	7:00-9:00; 14:00-17:00	0.1296$/kWh
	10:00-13:00; 18:00-22:00	0.1937$/kWh
Aviation fuel (kerosene) price	-	1.043$/L
Oxygen price	-	6.706 $/bottle (15MPa, 40L)/ 0.782$/kg
Carbon tax	-	20$/ton
Carbon emission factor	-	0.872kg/kWh

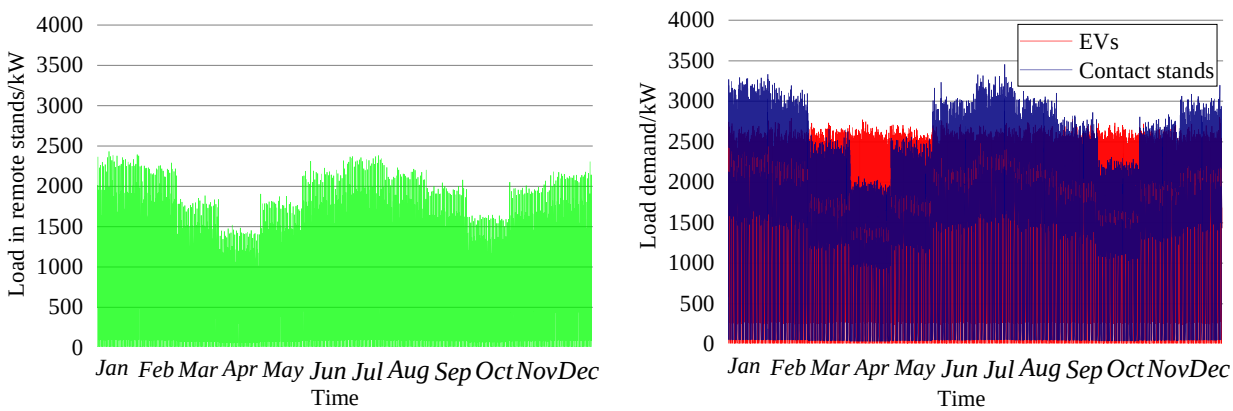

(a) Annual electric demand profile in remote stands (b) Annual electric demand of EVs and aircraft in contact stands

Fig. 9 Annual electric demand profile of airport microgrid energy system

The whole system costs of five different energy supply scenarios were compared to quantify the economic benefit of integrating solar-hydrogen-storage integrated energy system into airport.

The five energy system scenarios are described as follows:

Scenario #1: This is a reference scenario to assume that EVs and aircraft at contact stands are supplied by power grid. The aircraft at remote stands is powered by onboard APU.

Scenario #2: All aircraft (both contact and remote stands) and EVs are powered by power grid.

Scenario #3: The aircraft at contact stands and EVs are supplied by PV, BSS, and grid, while the aircraft at remote stands is supplied by onboard APU.

Scenario #4: All aircraft and EVs are powered by PV, BSS, and grid.

Scenario #5: Hydrogen production and storage are integrated into airport. The aircraft at contact stands and EVs are supplied by PV, BSS, and grid, while the aircraft at remote stands is supplied by mobile hydrogen fuel cell generation.

6. RESULTS AND DISCUSSION

6.1 Design results of airport energy system

This section shows the optimal sizing results of energy devices in different airport energy system scenarios with total annual investment, maintenance and operation costs in Table 3. Scenario 1 and 2 compare the electrification of aircraft APU at remote stands which will supply by only the grid, while Scenario 3 and 4 compares the electrification of aircraft APU at remote stands by PV, BBS and grid. Both comparisons indicate economic benefit in terms of overall cost reduction to electrify the aircraft APU at remote stands. By comparing with scenarios 4, scenario 5 introduces the hydrogen production and storage which will future reduce the total annual costs of airport energy system. The hydrogen energy system (HES) includes electrolyzer, HST and FC which offer carbon-free and mobility power generation to aircraft at remote stands, and to avoid the distribution network infrastructure at remote stands. Scenario 5 also shows the increased PV capacity and reduced BSS investment by integrating the hydrogen supply and storage into the airport energy system.

Table 3 Design results of airport energy system with five energy supply scenarios

Scenarios	PV(MW)	BSS(MW)	Electrolyzer (MW)	Hydrogen tank(kg)	Fuel cell (MW)	Total annual cost ($ million)
#1	-	-	-	-	-	6.379
#2	-	-	-	-	-	5.744
#3	17.908	24.1	-	-	-	4.926
#4	21.856	29.4	-	-	-	3.838
#5	33.951	17.8	7.5	1550	2.45	3.725

6.2 Cost breakdown analysis and carbon emissions

Figure 10 shows the breakdown costs for each scenario. The total annual cost is decomposed to investment, operation and maintenance (O&M) costs of energy devices, together with fuel and grid electricity costs, and emission costs. By comparing with scenario 1 (base case), the airport energy system with hydrogen integration (Scenario 5) is identified as the most cost-effective option, which can reduce the whole system costs by $2.654 million/year (41.6%). The PV +BSS system (Scenario 3) can reduce the costs by $1.453 million/year (22.78%). Further cost reduction by $1.088 million/year is observed when PV + BSS system is also expanded to aircraft at remote stands (Scenario 4). Through cost breakdown and comparison analysis, it can be seen that scenario 2 has the highest grid power purchase cost, while scenario 5 has the lowest grid cost. This indicates that PV + BSS + HES will minimize the grid dependence of airport energy supply, and thus reduce the infrastructure expansion and carbon emissions from the grid. In addition, scenario 5 has the highest investment costs due to the establishment of hydrogen production and storage devices, however, scenario 5 still appears to be the most economic solutions due to the lowest whole system costs by considering oxygen revenue. This shows that the investment costs of the HES can be compensated by offsetting other costs (such as grid and emissions costs, oxygen revenue etc.). Furthermore, the integration of HES leads to the significant increase in PV capacity, which makes the highest investment cost and O&M cost of both PV and hydrogen energy system in scenario 5. However, the revenue from oxygen sale at industrial and medical scales will compensate the high HES costs and encourage renewable PV integration, which makes the hydrogen energy system still an attractive option.

Fig. 11 shows the carbon emissions from grid and aircraft APU for each scenario. By comparing Scenario 1 and Scenario 2, the electrification of aircraft at remote stands (using grid supply to replace aircraft APU) has increased the carbon emissions on the grid side although the APU emission is eliminated. The carbon emissions on the grid side is consequently raised and lead to higher overall emissions, which is considered as a sub-optimal solution to just electrify aircraft APU and transfer the carbon emission sources from airport to the grid. In Scenarios 3 and 4, the installed PV generation not only reduces the carbon emissions inside the airport, but also reduces the emissions on the grid side due to the less grid power consumption. Scenario 5 has the lowest amount of carbon emissions, which indicates the environmental benefits of the hydrogen-solar-storage integrated energy system. Compared to scenario 1, carbon emissions in scenario 5 are reduced by 17,853.34 tons, while scenario 3 is reduced by 13,617.77 tons. It should be noted that the carbon emissions of Scenario 5 consider the worst environmental case that the hydrogen shortfall is compensated by the aircraft APU, however the carbon emissions of Scenario 5 are still the lowest due to the hydrogen as a decarbonized fuel.

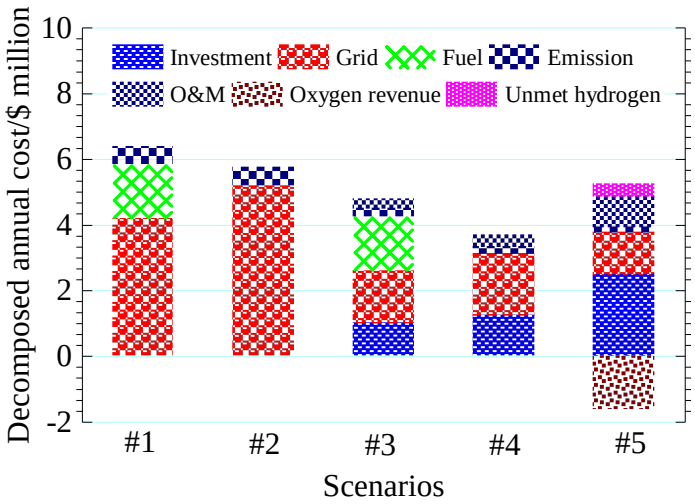

Fig. 10 Decomposed annual cost with five energy supply scenarios

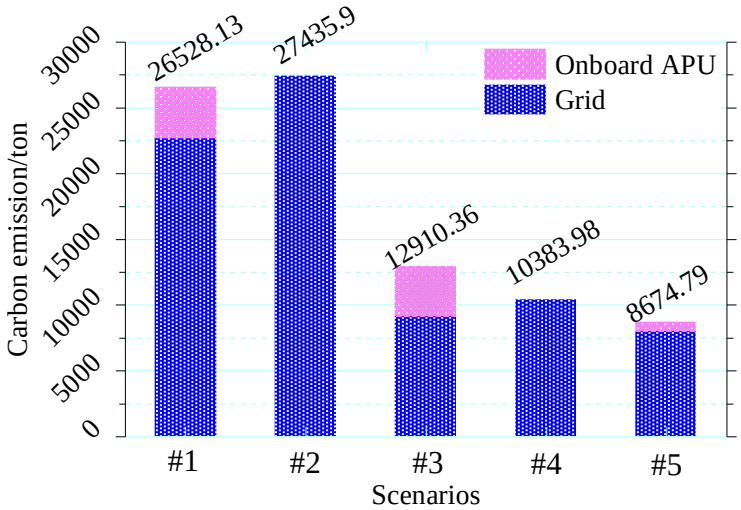

Fig. 11 Carbon emissions with five energy supply scenarios

6.3 Lifecycle investment cost analysis

In order to compare the costs of electrified airports with different scenarios, the annual costs including investment, operation costs, and emissions cost of airport energy system Scenario 2, Scenario 4, and Scenario 5 are shown in Fig.12. The costs are shown as the net present value. Scenario 4 and scenario 5 have large and upfront investment costs compared with scenario 2, but the operation and emissions cost are greatly reduced for the whole lifecycle of the project. In particular, PV accounts for a large proportion of the initial investment costs. The BSS is replaced twice during the entire lifecycle in the 10^{th} and 20^{th} years, respectively, and the FC in scenario 5 is replaced four times during the entire lifecycle in the 5^{th}, 10^{th}, 15^{th}, and 20^{th} years, respectively.

Cumulative costs over the lifecycle of the airport energy system for scenarios 2, 4, and 5 are compared in Fig. 13. The cumulative cost curve of scenario 5 is relatively flat with slower growth rate, because the operation cost of scenario 5 is

lower than scenario 4 due to oxygen revenue and lower emission costs. There are three breakeven years in accumulative cost compassion. The first breakeven year occurs in year 5.6, which indicates the scenario 2 will be cheaper than scenario 4 in the first 5.6 years due to the non-investment costs, however the accumulative costs in scenario 2 will be much higher than in scenario 4. If the project lifecycle has a short duration less than 5.6 years, the scenario 2 with only grid supply will be an ideal option for airport energy system design. The second breakeven year occurs in year 8.5, which indicates the scenario 5 with hydrogen integration will start gain benefits over the scenario 2 with grid supply. However, the hydrogen integration will still be more expensive than scenario 4. The last breakeven year occurs in year 20.5, which shows that the hydrogen integration will eventually have cost advantage over scenario 4 of PV+BSS system. Through analysis, it can be found that the integration of hydrogen into airport energy system has economic and environmental cost benefits in the long term.

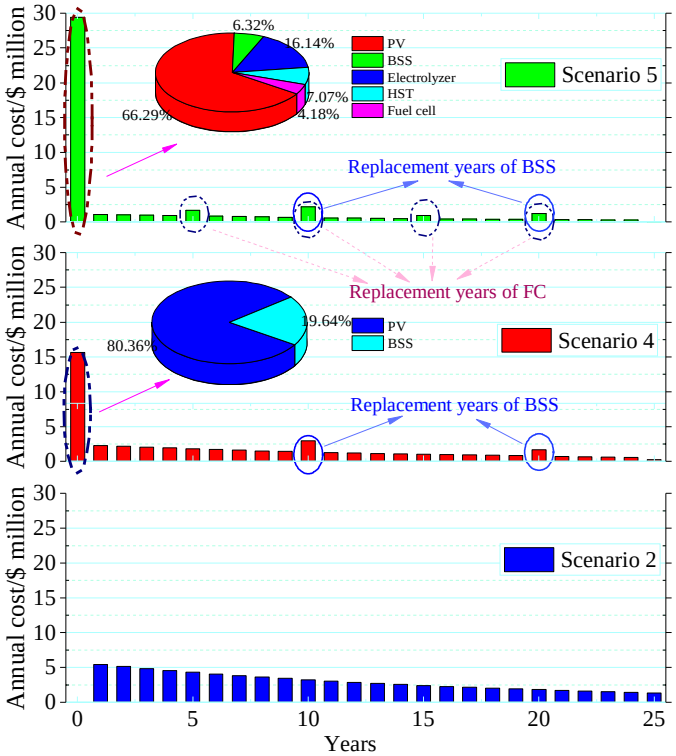

Fig. 12 Annual costs over the lifecycle of airport energy system in scenarios 2, 4, and 5

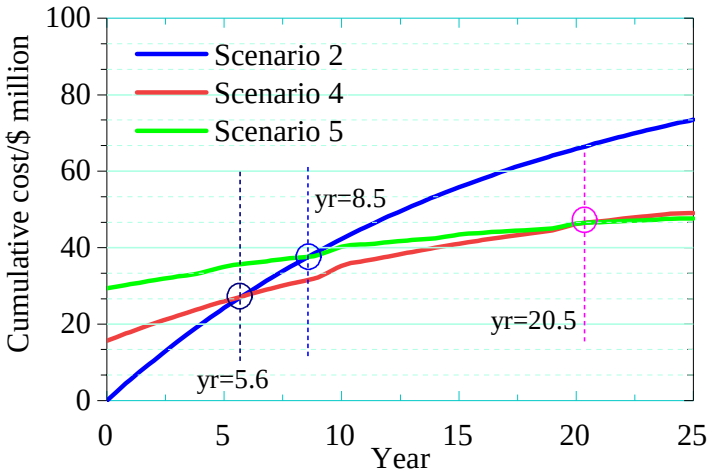

Fig. 13 Cumulative costs over the lifecycle of the airport energy system for scenarios 2, 4, and 5

6.4 Energy management strategies

This part shows the hourly energy dispatch simulation results of both electricity and hydrogen systems on a typical operation day. Fig. 14 shows the optimal electricity management strategies, and Fig. 15 illustrates the optimal hydrogen management strategies, both for scenarios 5 as an example. The positive values in these two figures are energy production (PV generation, grid electricity and hydrogen production) or the discharging of energy storage units (BSS and hydrogen storage), while the negative values are energy consumption (aircraft and EV loads, hydrogen consumption) or charging of energy storage. The BSS state-of-charge (SoC) and hydrogen stored level are also illustrated in these two figures.

It can be seen from Fig. 14 that the priority of PV energy supply is electric load, BSS, and HES in order. The PV energy is given priority to supply the load (8h), the excessive PV energy then charges the BSS (8h-10h), and the remaining PV energy that BSS cannot absorb then flows to the electrolyzer of HES to produce hydrogen (10h-19h). When PV energy is insufficient, the BSS discharges and supplies the electric load (20h-23h). When the BSS is insufficient, the DC microgrid system purchases power from the grid to supply the aircraft and EV load (1h – 7h, 24h).

As illustrated in Fig. 15, the fuel cell power generation closely follows the load of aircraft at remote stands. The hydrogen demand of FC is supplied by electrolyzer and hydrogen storage. It can be seen that due to the priority of PV energy consumption, the hydrogen demand of the fuel cell is firstly met by stored hydrogen (7h – 9h). When the excess PV energy flows to the HES, the electrolyzer starts to produce hydrogen for consumption by the fuel cell and the excess hydrogen is stored in the hydrogen storage tank (10h – 14h). When the hydrogen storage tank is full, the electrolyzer only produces hydrogen to supply the fuel cell (15h – 18h). If the additional PV energy is insufficient to meet the hydrogen demand of the fuel cell, the stored hydrogen is discharged from hydrogen storage tank (19h – 22h).

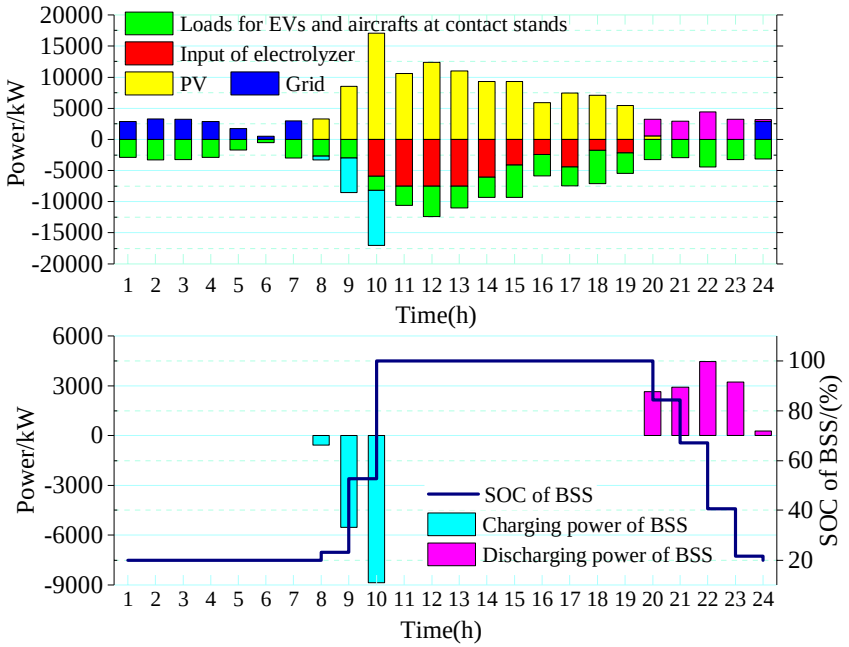

Fig. 14 Optimal electricity management strategy for scenario 5 on a typical day

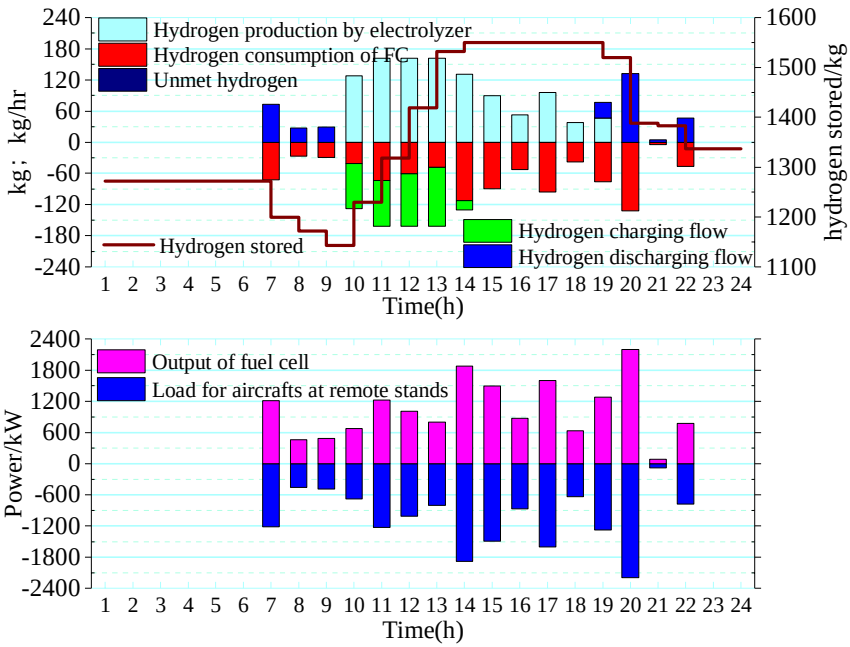

Fig. 15 Optimal hydrogen management strategy for scenario 5 on a typical day

6.5 Sensitivity analysis of key parameters

6.5.1 Annual solar irradiance

Fig. 16 shows the optimization results of the airport energy system for scenarios 2, 4, and 5 under different annual solar irradiance of PV generation. From the sensitivity analysis results shown in Fig. 16, Scenario 2 is not affected by solar irradiance because the airport is completely supplied by the grid. PV capacity of scenario 4 and scenario 5 are significantly

reduced when the solar irradiance becomes more intensive. Conversely, the BSS capacity requires to be expanded due to the increased fluctuation in PV by more intensive irradiance, in particular the BSS capacity for scenario 4 has reached the capacity limitation with the further increase of solar irradiance. With the increase of annual solar irradiance, the size of hydrogen energy system of scenario 5 decreases slightly, as more power will be provided by PV with higher solar irradiance. Therefore, the solar irradiance can effectively reduce the HES investment costs. In scenario 4 and 5, the total annual costs and carbon emissions are both reduced significantly with the increase of annual solar irradiance, this is due to the reduced PV investment costs and less electricity purchase from the grid with less grid emissions.

Fig. 16 (d) shows the cumulative cost curves for scenarios 2, 4, and 5 under the condition of maximum and minimum annual solar irradiance. It can be seen that cumulative costs of scenario 5 with HES is more sensitive to the solar irradiance comparing with scenario 4. With minimum solar irradiance, scenario 5 is no longer the most economic option as the scenario 4 with only PV+BSS has whole system costs lower through the entire project lifecycle. Therefore, it is recommended to adopt energy supply scenario 4 in low solar irradiance regions, while hydrogen energy system is recommended for the airports with high solar irradiance.

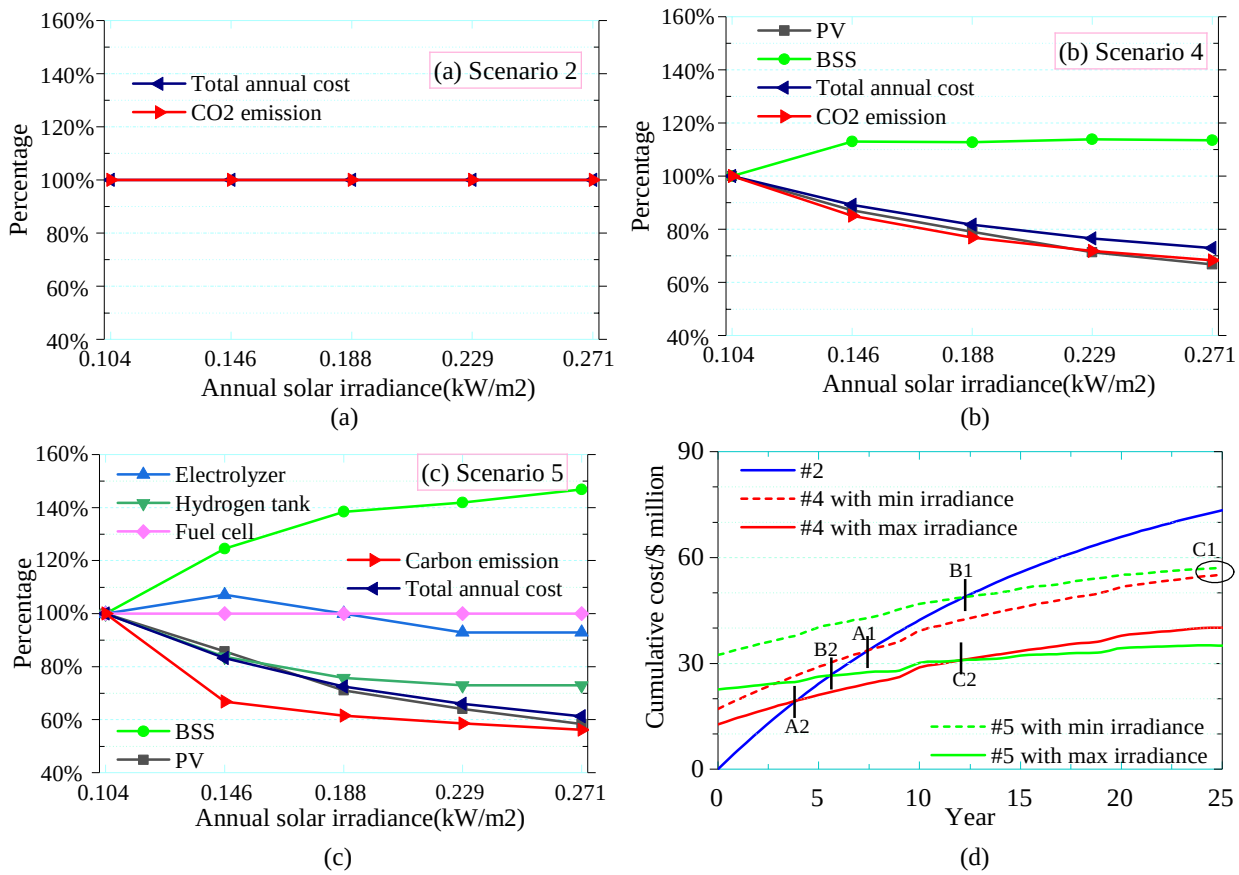

Fig. 16 (a)~(c) Sensitivity analysis for scenarios 2, 4, and 5 with different annual solar irradiance; (d) Cumulative costs for scenarios 2, 4, and 5 with max/min solar irradiance

6.5.2 Grid emission factor

Grid emission factor (kg/kWh) is the carbon emission associated with each unit of electricity produced by the grid. Fig. 17 shows the sensitivity analysis of grid emission factor on the airport energy system design for scenario 2, 4, and 5. Grid emission factor is changed from its current value 0.872 kg/kWh to 0 kg/kWh, representing a decarbonizing trend to a future zero emission grid. In all energy supply scenarios, grid emission factor plays an important role in reducing CO2 emissions of airport energy system towards low-carbon aviation targets. However, the total annual costs only reduce by 5% as the emission costs are small part of whole system costs which mainly consists of investment, operation and maintenance costs. When the grid emission reduces, the PV+BSS system capacity will drop by up to 20% in scenario 5 while the HES capacity will expand slightly, which indicates the grid emissions will impact the energy share between the PV, BSS and HES.

Fig. 19 shows the cumulative cost curves for scenarios 2, 4, and 5 under current and zero grid carbon emissions. In each scenario, it is clearly indicated that the low-carbon grid will lead to a lower whole system cumulative costs over the entire lifecycle of the project (from solid line to dot line). Regardless of grid emission factor, the scenario 5 with HES integration will still demonstrate as an economic solution in long-term by comparing with other energy supply scenarios.

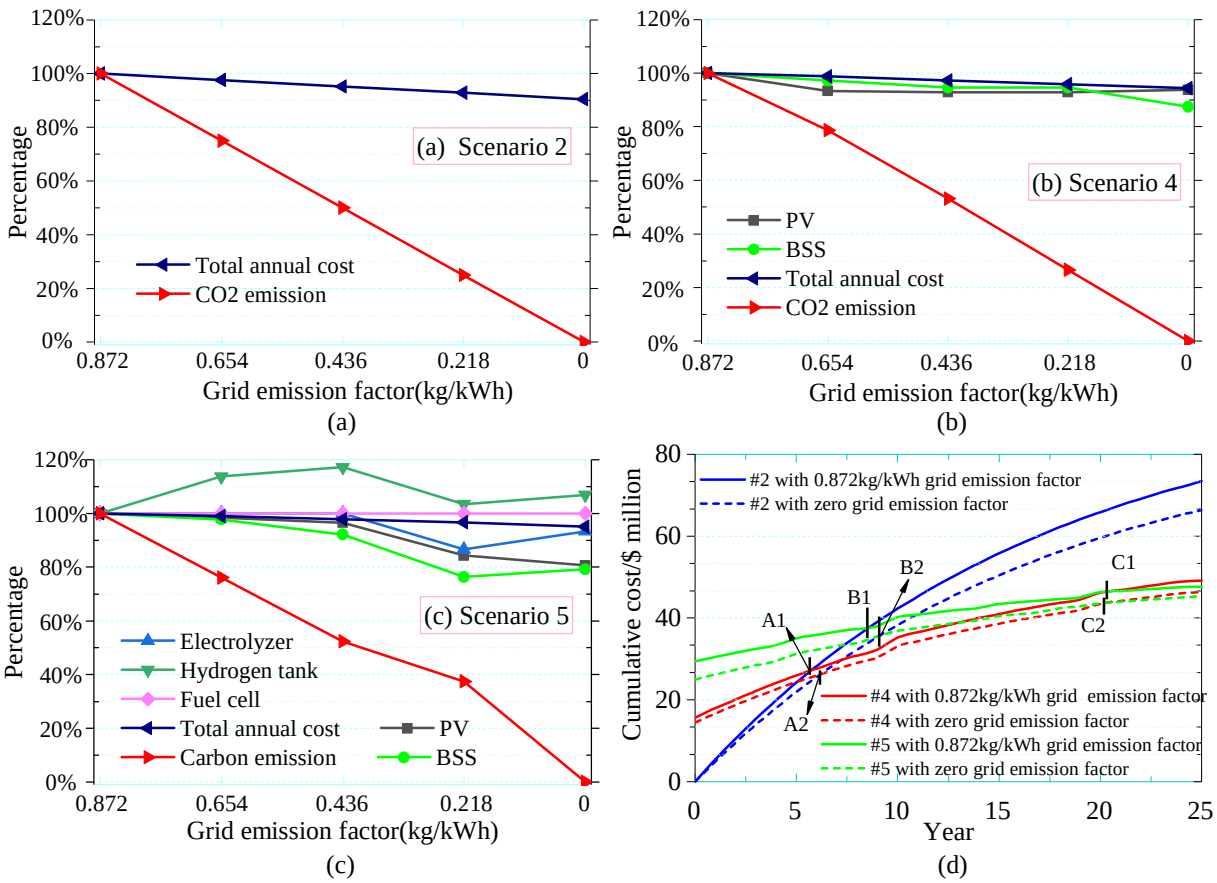

Fig. 17 (a)~(c) Sensitivity analysis for scenarios 2, 4 and 5 with different grid emission factors; (d) Cumulative costs for scenarios 2, 4, and 5 with 0.872kg/kWh and zero grid emission factors

6.5.3 Electricity prices

Fig. 18 shows the electricity prices can significantly impact the airport energy system design with associated CO2 emissions and total annual costs. The total annual costs of Scenario 2 with only grid supply has a linear trend against the electricity price, but CO2 emission stays constant regardless of electricity price variation. This is due to the airport energy system of scenario 2 is only supplied by grid electricity. Scenario 4 and 5 show that PV, BSS and HES capacities are all sensitive to the electricity price change. For example, when the grid electricity price drops, the capacities of other energy devices are reduced accordingly. This is due to the energy dispatch of more grid electricity which is cheaper than local energy supply. As a result, the CO2 emissions will raise due to grid electricity usage leading to higher grid carbon emissions. When the electricity price becomes cheaper, the total annual costs of the whole system reduces significantly. This becomes an extreme case in Fig. 18 (d) when the electricity price drops to 40%, the scenario 2 tends to become an economic solution that only use grid electricity to supply the airport energy system, while PV+BSS+HES integration become a less competitive option.

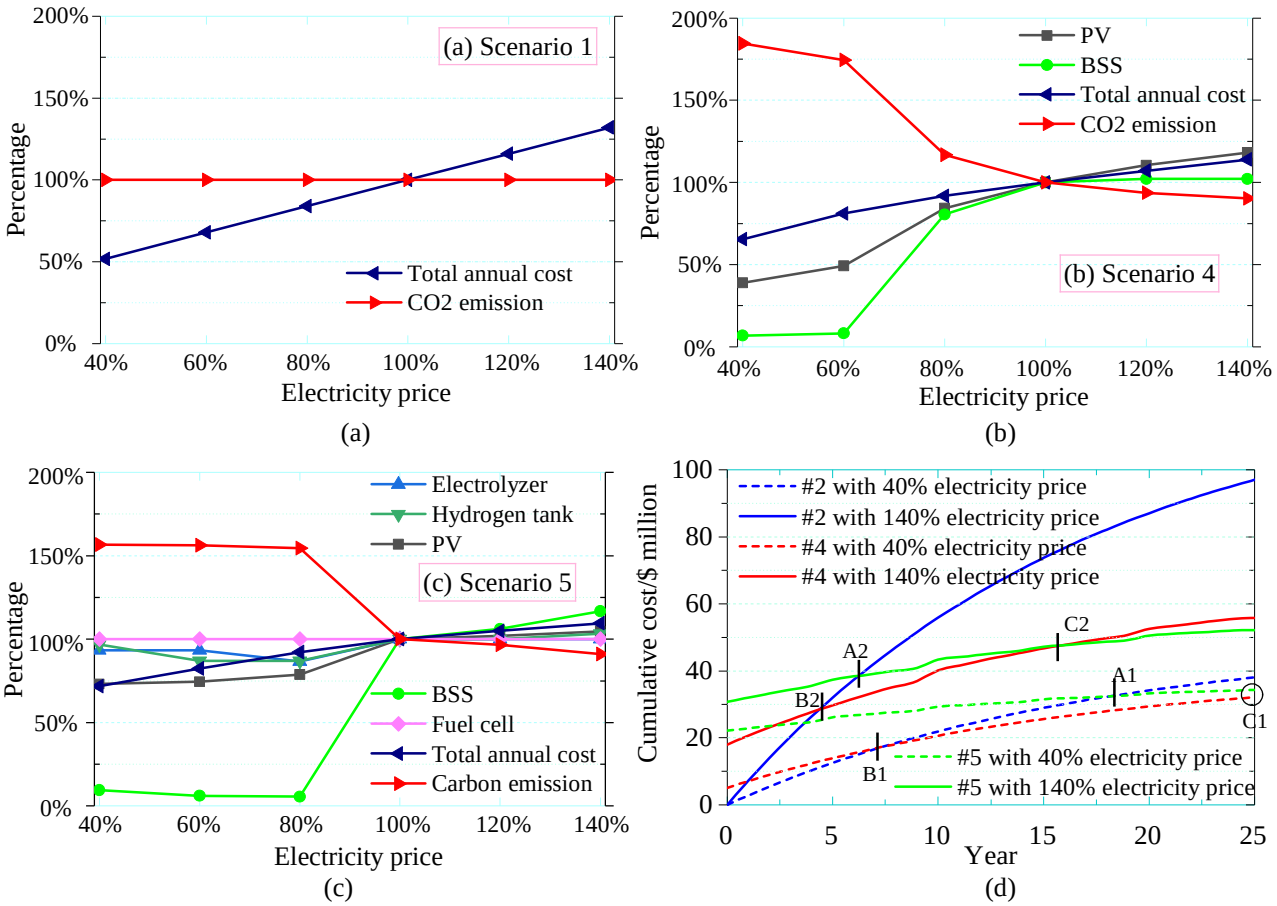

Fig. 18 (a)~(c) Sensitivity analysis of electricity prices on energy system design in scenarios 2, 4, and 5; (d) Cumulative costs for scenarios 2, 4, and 5 with 40% and 140% electricity prices

6.5.4 Carbon tax

Fig. 19 shows the optimization results of the airport energy system for scenario 2, 4, and 5 under different carbon tax ($/ton). With the increase of carbon tax, the total annual costs of scenario 2 that is solely supplied by the grid increases linearly, while carbon emissions remain unchanged. In scenario 4 and 5, higher carbon tax leads to higher total annual costs, and the substantial increase in the PV+BSS and HES capacities to reduce the grid electricity usage. Such system alternation results in a substantial reduction in CO2 emissions which are heavily charged by higher carbon tax.

Fig. 19 (d) shows the cumulative cost curves for scenarios 2, 4, and 5 with the carbon tax of 20$/ton and 100$/ton. Scenario 2 with only grid supply is highly sensitive to the carbon tax, with the cumulative costs increasing significantly by the higher carbon tax. The Scenario 5 with HES integration can better hedge the risks of carbon tax increase, as the cumulative costs of scenario 5 become the lowest at the end of project lifecycle under both high and low carbon taxes.

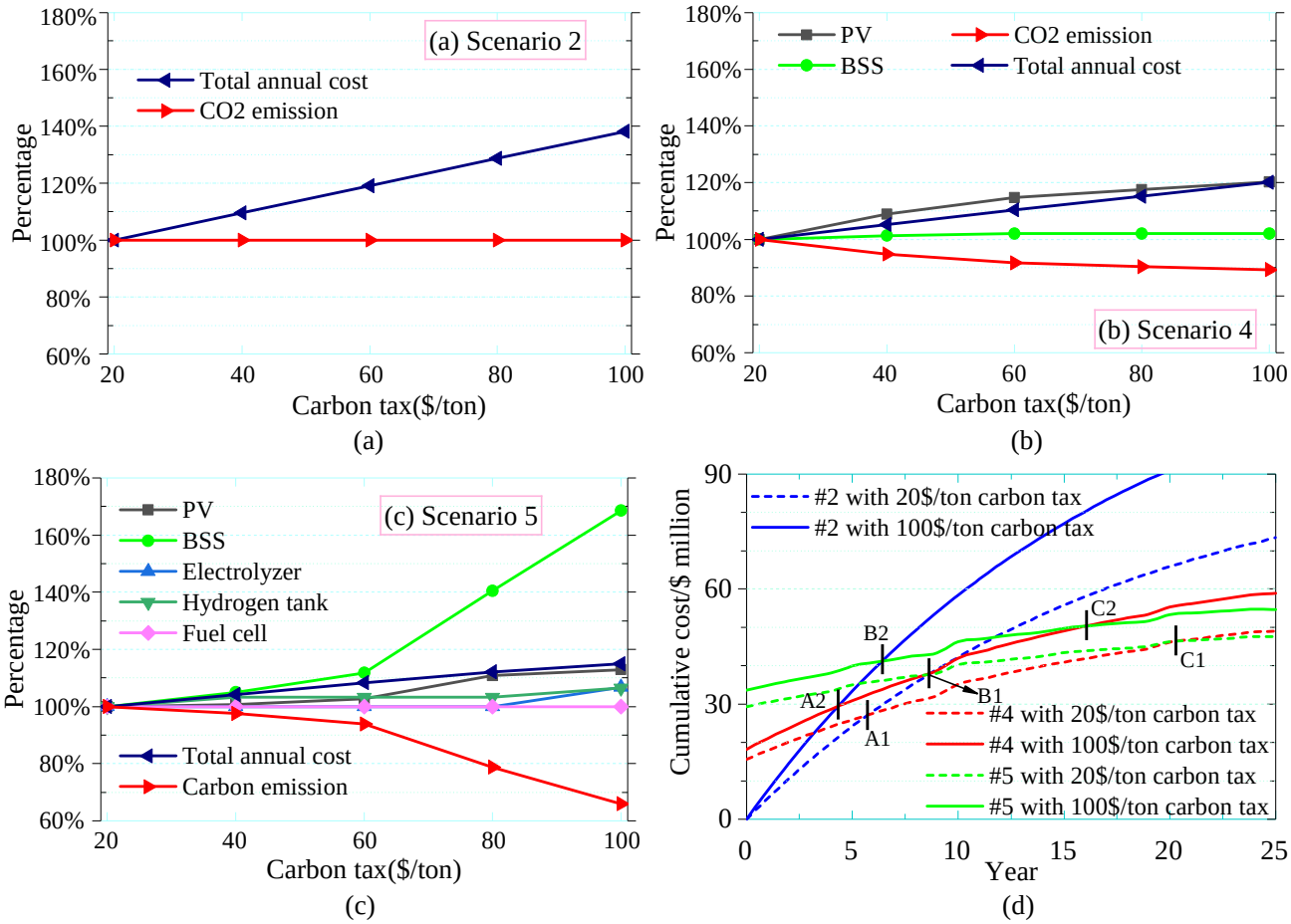

Fig. 19 (a)~(c) Sensitivity analysis of carbon tax on the energy system design for scenarios 2, 4, and 5; (d) Cumulative costs for scenarios 2, 4, and 5 with 20$/ton and 100$/ton carbon tax

6.5.5 Unit investment cost of hydrogen energy system

A major constraint on the integration of HES into airport energy system is its high investment costs. This section analyzes the unit investment cost of HES in affecting the airport energy system design with associated economic and environmental assessment. In the sensitivity analysis of HES unit investment costs, the electrolyzer, HST, and FC are scaled up or down by the same proportion. Fig. 20 (a) shows that the sizes of both electrolyzer and the hydrogen storage tank will increase when the unit investment cost of hydrogen energy system reduces from 140% to 60%. The installation capacity of the fuel cell remains constant due to the maximum APU load at the remote stands that determines the fuel cell capacity. In particular, the capacity of hydrogen storage tank expands significantly due to the lower unit investment cost that enabling the hydrogen storage to be a viable option. As the HES becomes a more cost competitive option, the capacity of PV is decreased by up to 10%. Finally, the total annual cost of the whole system continues to decline due to the reduction in HES investment costs.

Fig. 20 (b) shows the cumulative cost curves under different HES unit costs of 60%, 100% and 140%. If the unit cost of HES increases, the scenario 5 of HES integration will be no longer the cheapest energy supply options. As a result, the reduction in unit investment cost of HES is an effective way to encourage hydrogen integration into airport energy systems.

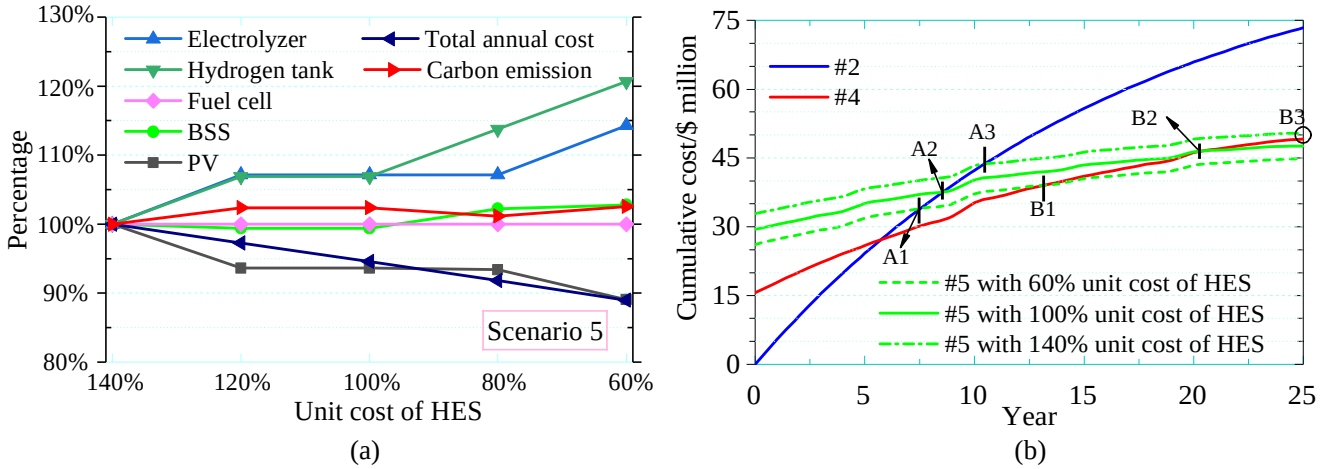

Fig. 20 (a) Sensitivity analysis of HES unit investment cost on energy system design for scenario 5; (b) Cumulative costs for scenarios 2, 4, and 5 with 60%, 100%, and 140% unit investment costs of HES

6.5.6 Operation benefits with different oxygen prices

As shown in Fig. 21, oxygen price has a significant impact on the cumulative costs of scenario 5, which mainly affects the operation costs through the oxygen sale revenue. When the oxygen price is high, the scenario 5 has a reduced cumulative cost along the project timeline, larger cost saving can be observed towards the end of project lifecycle due to the sale of oxygen as a commercial product. In contrast, the HES integration will become a less economic option if the oxygen price drops to 60% due to the less revenue can be made from the oxygen sale.

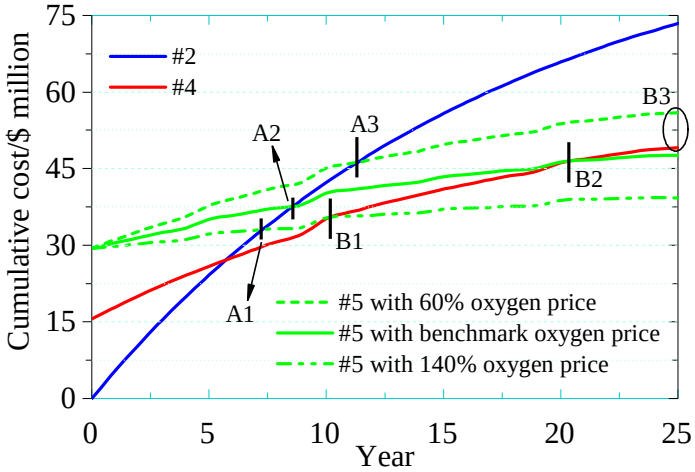

Fig. 21 Cumulative costs for scenarios 2, 4, and 5 with different oxygen prices

7. CONCLUSION

This paper conducts the techno-economic analysis of hydrogen-solar-storage integrated energy system for airport electrification. The key energy resources including photovoltaic, hydrogen energy system, electric vehicles, hydrogen fuel cell generator, and battery storage system are integrated to form a direct current microgrid with various energy supply options. Based on the flight schedules, an aircraft load characteristic model is developed to quantify the electric aircraft load by replacing the aircraft auxiliary power unit. A vehicle matrix method with sequencing algorithm is proposed to generate electric vehicles charging load profile in airport operation. Then, a mixed integer liner programming optimization method is developed to optimally design the capacity of each energy devices of airport microgrid, with the objective to minimize the total annual costs of the whole energy system including investment, operation and emission costs during the lifecycle of the project. Energy management strategies is developed to hourly dispatch photovoltaic generation, grid electricity purchase, battery charging / discharging, and hydrogen production / storage to meet the supply-demand balance of airport microgrid. Five airport energy system scenarios are proposed to compare the different energy supply options with associated techno-economic and environmental assessment of each different microgrid solution. Sensitivity analysis is conducted to evaluate the impacts of key parameters of solar irradiance, grid emission, electricity price, carbon tax, hydrogen unit cost and oxygen sale price on the design, costs and operation of the proposed microgrid. The case studies demonstrate the techno-economic benefits of hydrogen energy system integration into airport with renewable power generation and storage. The key findings are summarized as follows:

1) The integrated hydrogen-solar-storage system proposes an economic and environment friendly solution to design and operate the future airport energy system, with total annual energy system cost saving and emissions reduction by 41.6% and

67.29%, respectively.

2) Due to the high upfront investment costs of the hydrogen energy system, the airport energy system integrated with hydrogen production and storage facilities has high initial cumulative costs comparing with other microgrid designs. However, the hydrogen energy system will provide sufficient economic and environmental benefits in the long term towards the project lifecycle.

3) Sensitivity analysis shows that the higher solar irradiance, the lower hydrogen unit investment cost, and higher oxygen price will lead to the more economic and environmental benefits of the hydrogen energy system integration. Hydrogen energy system is able to hedge the uncertainties against electricity price, grid emission and carbon tax.

ACKNOWLEDGEMENTS

This work was supported by UK EPSRC Supergen Energy Networks Hub Flexible Fund (SENFC1-023); UK Department for Transport Transport-Technology Research Innovation Grant (T-TRIG); National Natural Science Foundation of China International Visiting Program (51807127) for Excellent Young Scholars of Sichuan University.

REFERENCES

[1] IEA, 2018. CO2 Emissions Statistics 2018 accessed 15 January 2019. https://www.iea.org/stati stics/co2emissions/.
[2] Soutter A R B, Mottus R. “Global warming” versus “climate change”: A replication on the association between political self-identification, question wording, and environmental beliefs. Journal of Environmental Psychology 2020; in press.
[3] European Commission, “Flightpath 2050: Europe’s Vision for Aviation”, Report of the high-level group on aviation research, publications office of the European Union, Luxembourg, 2011
[4] CAAC. "13th Five-Year Plan" for civil aviation energy conservation and emission reduction. http://www.caac.gov.cn/big5/www.caac.gov.cn/XXGK/XXGK/ZCFBJD/201702/P020170228618181713499.pdf.
[5] Benjamin J.B, Joaquim R.R.A.M. Electric, hybrid, and turboelectric fixed-wing aircraft: A review of concepts, models, and design approaches. Progress in Aerospace Sciences 2019; 104:1-19.
[6] Sun MY, Cremer J, Strbac G. A novel data-driven scenario generation framework for transmission expansion planning with high renewable energy penetration. Applied Energy 2018; 228:546-555.
[7] Shiarishi K, Shirley R, Kammen D. Geospatial multi-criteria analysis for identifying high priority clean energy investment opportunities: A case study on land-use conflict in Bangladesh. Applied Energy 2019; 235:1457-1467.
[8] Dong PF, Yi LZ, Li HJ, Li G. Analysis of capacity-increasing and line loss of simultaneous AC-DC transmission. Chinese Journal of Power Source 2017;41(01): 142-145.
[9] CAACNEWS. Beijing Daxing International Airport: Renewable energy accounts for more than 10%. http://www.caacnews.com.cn/1/5/201812/t20181213_1262825.html.
[10] Zhang J, Cho H, Luck R, J.Mago P. Integrated photovoltaic and battery energy storage (PV-BES) systems: An analysis of existing financial incentive policies in the US. Applied Energy 2018; 212:895-908.
[11] Sgobbi A, Nijs W, Miglio R, Chiodi A, Gargiulo, Thiel Christian. How far away is hydrogen? Its role in the medium and long-term decarbonisation of the European energy system. International Journal of Hydrogen Energy 2016;41:19-35.
[12] Dawood F, Anda M, G. M. Shafiukkah. Hydrogen production for energy: An overview. International Journal of Hydrogen Energy 2020; 45(7): 3847-3869.

[13] Eriksson E.L.V, Gray E.M. Optimization and integration of hybrid renewable energy hudrogen fuel cell energy system - A critical review. Applied energy 2017; 202:348-364.
[14] Widera B. Renewable hydrogen implementations for combined energy storage, transportation and stationary applications. Thermal Science and Engineering Progress 2020; 16:100460.
[15] Münster M, Sneum DM, Bramstoft R, Bühler F, Elmegaard B, Giannelos S, et al. Sector Coupling: Concepts, State-of-the-art and Perspectives. 2020.
[16] Yang Y, Zhang S, Xiao Y. An MILP model for optimal design of district-scale distributed energy resource systems. Energy 2015;90:1901-1915.
[17] Quashie M, Marnay C, Bouffard F, Joós G. Optimal planning of microgrid power and operating reserve capacity. Applied Energy 2018; 210: 1229-36.
[18] Patrizia S, Gioacchino N, Gellio C. Planning and design of sustainable smart multi energy systems. The case of a food industrial district in Italy. Energy 2018;163:443-56.
[19] Ma TF, Wu JY, Hao LL, Lee WJ, Yan HG, Li DZ. The optimal structure planning and energy management strategies of smart multi energy system. Energy 2018;160:122-41.
[20] Benjamin Lux, Benjamin Pfluger. A supply curve of electricity-based hydrogen in a decarbonized European energy system in 2050. Applied Energy 2020; 269:115011.
[21] Cardona E, Piacentino A, Cardona F. Energy saving in airports by trigeneration. Part I: Assessing economic and technical potential. Applied Thermal Engineering 2006; 1427-1436.
[22] Cardona E, Sannino P, Piacentino A, Cardona F. Energy saving in airports by trigeneration. Part II: Short and long term planning for the Malpensa 2000 CHCP plant. Applied thermal Engineering 2006; 1437-1447.
[23] Zhang Y, Si PF, Feng Y, Rong XY, Wang X, Zhang YP. Operation strategy optimization of BCHP system with thermal energy storage: A case study for airport terminal in Qingdao, China. Energy and Buildings 2017; 165: 464-478.
[24] Kılkıs B, Kılkıs S. New exergy metrics for energy, environment, and economy nexus and optimum design model for nearly-zero exergy airport (nZEXAP) systems. Energy; 140: 1329-1349.
[25] KilKis B, KilKis S, KilKis S. Central air with ice storage for parked planes at the terminal gate: exergy, energy, and economy perspectives. International Journal Sustainable Aviation 2017.
[26] Sikorski E. Air-conditioning of parked aircraft by ground based equipment. International Refrigeration and Air Conditioning Conference at Purdue, July 12-15, 2010. Paper No 2039.
[27] Chen CY, Sun ZP, Ju C. Application of energy storage power station technology in airport field. Modern Architecture Electric 2019; 10(02):52-55.
[28] Sreenath S, Sudhakar K, Yusop A.F, Solomin E, Kirpichnikova. Solar PV energy system in Malaysian airport: Glare analysis, general design and performance assessment. Energy Reports 2020; 6:698-712.
[29] Sreenath S, Sudhakar K, Yusop A.F. Solar photovoltaics in airport: Risk assessment and mitigation strategies. Environmental Impact Assessment Review 2020; 84:106418.
[30] Yu JL. Analysis on the Emission Reduction Potential of "Oil to Electricity" for Airport Ground Vehicles and Its Implementation. Energy and Environment 2017;2;30-31+36.
[31] Silvester S, Beella S. k, Timmerem A. V, Bauer P, Quist J, Dijk S. Exploring design scenarios for large-scale implementation of electric vehicles; the Amsterdam Airport Schiphol case. Journal of Cleaner Production 2013;48:211-219.
[32] Yang Y, Liu YB, Huang Y, Wang XD.. Research on allocation of off-grid photovoltaic-storage system considering APU electric energy substitution in civil aviation airport. Power Demand Side Management 2020;22(03):19-25.
[33] AFAR. This Is the First U.S. Airport to Be Fully Solar-Powered. https://www.afar.com/magazine/this-is-the-first-us-airport-to-be-fully-solar-powered. 2019.
[34] CPH. Copenhagen Airport's solar power system inaugurated. https://www.cph.dk/en/about-cph/press/news/2014/9/copenhagen-airports-solar-power-system-inaugurated/. 2014.
[35] Apostolou D. Optimisation of a hydrogen production–storage–repowering system participating in electricity and transportation markets. A case study for Denmark. Applied Energy 2020; 265: 114800.
[36] Seo Sk, Yun DY, C J Lee. Design and optimization of a hydrogen supply chain using a centralized storage model. Applied energy 2020; 262: 114452.

[37] AINouss A, McKay G, AI-Ansari T. Enhancing waste to hydrogen production through biomass feedstock blending: A techno-economic-environmental evaluation. Applied energy 2020; 266: 114885.
[38] Farahani S, Bleeker C, Wijk A, Lukszo Z. Hydrogen-based integrated energy and mobility system for a real-life office environment. Applied energy 2020; 264: 114695.
[39] Wu X, Qi SX, Wang Z, Duan C, Wang XL, Li FR. Optimal scheduling for microgrids with hydrogen fueling stations considering uncertainty using data-driven approach. Applied energy 2019; 253: 113568.
[40] Qiu Y, Zhou SY, Wang JH, Chou J, Fang YH, Pan GS. Feasibility analysis of utilising underground hydrogen storage facilities in integrated energy system: Case studies in China. Applied energy 2020; 269: 115140.
[41] Clean Intralogistics Net. Plug Power and MULAG to Bring New Hydrogen-Powered Ground Support Vehicles to Hamburg Airport. http://www.cleanintralogistics.net/portfolio-item/plug-power-and-mulag-to-bring-new-hydrogen-powered-ground-support-vehicles-to-hamburg-airport/, 2019.
[42] The Constructor. Components of an Airport, https://theconstructor.org/transportation/airport-components/20033/; 2016.
[43] FCX System. Why the aviation industry operates on 400 HZ power, https://fcxinc.com/why-the-aviation-industry-operates-on-400-hz-power/;2016.
[44] ACTIONPOWER. Remote aircraft power supply solution, http://www.cnaction.com/CivilGPDDetail_2727.html; 2020.
[45] Vossos V, Gerber D, Bennani Y, Brown R, Marnay C. Techno-economic analysis of DC power distribution in commercial buildings. Applied energy 2018; 230: 663-678.
[46] Justo J J, Mwasilu F, Lee J, Jung JW. AC-microgrids versus DC-microgrids with distributed energy resources: A review. Renewable and Sustainable Energy Reviews 2013; 24:387-405.
[47] Feng W, Jin M, Liu X, Bao Y, Marnay C, Yao C, et al. A review of microgrid development in the United States – A decade of progress on policies, demonstrations, controls, and software tools. Applied energy 2018; 228:1656-1668.
[48] Xu L, Ruan X, Mao C, Zhang B, Luo Y. An improved optimal sizing method for wind-solar-battery hybrid power system. IEEE Transactions on Sustainable Energy 2013; 4(3): 774-785.
[49] Niitta N, Wu FX, Lee JT, Yushin G. Li-ion battery materials: present and future. Materials Today 2015; 18(5):252-264.
[50] Xiang Y, Cai HH, Gu CH, Shen XD. Cost-benefit analysis of integrated energy system planning considering demand response. Energy 2020; 192: 116632.
[51] Nehrir M. H, Wang C. Modeling and control of fuel cells: distributed generation applications. John Wiley & Sons, 2009.Chapter 2.
[52] Toghyani S, Fakhradini S, Afshari E, Baniasadi E, Jamalabadi MYA, Shadloo MS. Optimization of operating parameters of a polymer exchange membrane electrolyzer. International Journal of Hydrogen Energy 2019; 44(13): 6403-6414.
[53] Yu J, Shi QY, Yang ZF, Dai W, Wang XB. Day-ahead scheduling method of P2G system considering operation characteristics of electrolyzed water and methanation unit. Automation of Electric Power System 2019; 43(18): 18-28.
[54] Zhang Y, Wei W. Model construction and energy management system of lithium battery, PV generator, hydrogen production unit and fuel cell in islanded AC microgrid. International Journal of Hydrogen Energy 2020; in press.
[55] Chengdu shuangliu international airport. Flight Information, http://www.cdairport.com/en/flightInfor.aspx?t=113; 2020.
[56] Gulan K, Cotilla-Sanchez E, Cao Y. Charging analysis of ground support vehicle in an electrified airport. 2019 IEEE Transportation Electrification Conference and Expo (ITEC) 2019.
[57] Fu P, Pudjianto D, Zhang X, Strbac G. Integration of hydrogen into multi-energy systems optimization. Energies 2020; 13(7): 1606.
[58] Brka A, Al-Abdeli Y, Kothapalli G. Predictive power management strategies for stand-alone hydrogen systems: Operational impact. International Journal of Hydrogen Energy 2016; 41(16): 6685-6698.
[59] Electricity sales price list. https://wenku.baidu.com/view/94c64b2381c758f5f61f67d9.html, 2018.
[60] Takahashi K, Louhisuoiges M. IGES List of Grid Emission Factors, Institute for Global Environmental Strategies, v10.9; 2020.

Techno-economic design of energy systems for airport electrification: a hydrogen-solar-storage integrated microgrid solution

Xiang, Yue

2021-01-02

Xiang Y, Cai H, Liu J, Zhang X. (2021) Techno-economic design of energy systems for airport electrification: A hydrogen-solar-storage integrated microgrid solution. Applied Energy, Volume 283, February 2021, Article number 116374

https://doi.org/10.1016/j.apenergy.2020.116374